HAL
open science

Biosignature Analysis of Mars Soil Analogs from the Atacama Desert: Challenges and Implications for Future Missions to Mars

Joost W Aerts, Andreas Riedo, Daniel J Melton, Simone Martini, Jessica Flahaut, Uwe Meierhenrich, Cornelia Meinert, Iuliia Myrgorodska, Robert Lindner, Pascale Ehrenfreund

To cite this version:

Joost W Aerts, Andreas Riedo, Daniel J Melton, Simone Martini, Jessica Flahaut, et al.. Biosignature Analysis of Mars Soil Analogs from the Atacama Desert: Challenges and Implications for Future Missions to Mars. Astrobiology, In press, 10.1089/ast.2019.2063 . hal-02526134

HAL Id: hal-02526134

https://hal.univ-cotedazur.fr/hal-02526134v1

Submitted on 2 Apr 2020

HAL is a multi-disciplinary open access archive for the deposit and dissemination of scientific research documents, whether they are published or not. The documents may come from teaching and research institutions in France or abroad, or from public or private research centers.

L'archive ouverte pluridisciplinaire **HAL**, est destinée au dépôt et à la diffusion de documents scientifiques de niveau recherche, publiés ou non, émanant des établissements d'enseignement et de recherche français ou étrangers, des laboratoires publics ou privés.

ASTROBIOLOGY
Volume 20, Number 6, 2020
© Mary Ann Liebert, Inc.
DOI: 10.1089/ast.2019.2063

Research Article

Biosignature Analysis of Mars Soil Analogs from the Atacama Desert: Challenges and Implications for Future Missions to Mars

Joost W. Aerts,[1] Andreas Riedo,[2] Daniel J. Melton,[2] Simone Martini,[2] Jessica Flahaut,[3] Uwe J. Meierhenrich,[4] Cornelia Meinert,[4] Iuliia Myrgorodska,[5] Robert Lindner,[6] and Pascale Ehrenfreund[2]

Downloaded by UPPSALA UNIVERSITETSBIBLIOTEK from www.liebertpub.com at 03/16/20. For personal use only.

Abstract

The detection of biosignatures on Mars is of outstanding interest in the current field of Astrobiology and drives various fields of research, ranging from new sample collection strategies to the development of more sensitive detection techniques. Detailed analysis of the organic content in Mars analog materials collected from extreme environments on Earth improves the current understanding of biosignature preservation and detection under conditions similar to those of Mars. In this article, we examined the biological fingerprint of several locations in the Atacama Desert (Chile), which include different wet and dry, and intermediate to high elevation salt flats (also named salars). Liquid Chromatography and Multidimensional Gas Chromatography Mass Spectrometry measurement techniques were used for the detection and analysis of amino acids extracted from the salt crusts and sediments by using sophisticated extraction procedures. Illumina 16S amplicon sequencing was used for the identification of microbial communities associated with the different sample locations. Although amino acid load and organic carbon and nitrogen quantities were generally low, it was found that most of the samples harbored complex and versatile microbial communities, which were dominated by (extremely) halophilic microorganisms (most notably by species of the Archaeal family *Halobacteriaceae*). The dominance of salts (*i.e.*, halites and sulfates) in the investigated samples leaves its mark on the composition of the microbial communities but does not appear to hinder the potential of life to flourish since it can clearly adapt to the higher concentrations. Although the Atacama Desert is one of the driest and harshest environments on Earth, it is shown that there are still sub-locations where life is able to maintain a foothold, and, as such, salt flats could be considered as interesting targets for future life exploration missions on Mars. Key Words: Mars—Atacama Desert—Biosignatures—Amino acids—Microbial communities—Organic carbon. Astrobiology 20, xxx–xxx.

1. Introduction

Gaining more insight into the geological and potential biological history of Mars is still a major goal for the planetary community. Although the past few decades of study have supplied us with large amounts of scientific data regarding mineralogy, geological record, current and past environmental conditions (including those that could support life), and the presence of water and even of organic molecules on Mars, more questions remain. Many of these questions can only be directly addressed by *in situ* research on the Red Planet itself. However, Mars exploration missions are expensive, complex, and time consuming. Therefore, the amount and type of research that can be done on the Red Planet itself is still limited. However, certain terrestrial environments can serve as analogs for selected, past martian environments.

One of the most stringent questions is, of course, whether there is, or has been, life on Mars. This leads to follow-up questions such as: How to look for signs of (extinct) life? Which type of biosignatures are appropriate targets (stability vs. diagnostic power)? Where would chances be highest of

[1]Molecular Cell Biology, Faculty of Science, VU University Amsterdam, Amsterdam, The Netherlands.
[2]Astrobiology Laboratory, Sackler Laboratory for Astrophysics, Leiden Observatory, Leiden University, Leiden, The Netherlands.
[3]CRPG, CNRS/University of Lorraine, Vandoeuvre-les-Nancy, France.
[4]CNRS, Institut de Chimie de Nice UMR 7272, Université Côte d'Azur, Nice, France.
[5]School of Chemistry, University of Bristol, Bristol, United Kingdom.
[6]Life Support and Physical Sciences Instrumentation Section, European Space Agency, ESTEC, Noordwijk, The Netherlands.

finding such biomarkers? To increase the chances for successful detection, it is important to assess these questions to the best of our abilities. In this regard, a great deal of information can be acquired by investigating terrestrial Mars analog environments.

One of the most famous and well-studied Mars analog environments is the Atacama Desert in Chile. The Atacama Desert is known as the driest, nonpolar desert on Earth, receiving only a few millimeters of rain per year on average (Clarke, 2006). The region in the northern part of Chile and the Central Andes, which encompasses the Atacama Desert, contains a multitude of north to south trending mountain ranges and closed basins, of which the central parts are often filled with evaporite deposits or, in more rare cases, highly saline waters (collectively known as salars) (Fig. 1). Due to the desiccated conditions and lack of significant weathering effects, salts have accumulated in the region over the course of millions of years, resulting in the presence of an overall high salinity in the local soils (Michalski *et al.*, 2004).

Common salts/evaporites found in the Atacama Desert include halite, gypsum, anhydrite, borates, sodium sulfates, and perchlorate salts (Stoertz and Ericksen, 1974; Ericksen, 1981; Böhlke *et al.*, 1997; Flahaut *et al.*, 2017). The Atacama Desert has an average temperature of 11–16°C with strong fluctuations during day or night, and with elevation (Stoertz and Ericksen, 1974; McKay *et al.*, 2003; Clarke, 2006; Gómez-Silva *et al.*, 2008). It is believed to be the oldest desert on Earth, with extreme arid conditions persisting for at least 10–15 million years (Ericksen, 1983; Berger and Cooke, 1997; Clarke, 2006). The region is also exposed to the highest doses of ultraviolet (UV) radiation found on Earth (Cordero *et al.*, 2018), and oxidizing conditions are commonly found in the desert soils (Navarro-Gonzalez *et al.*, 2003). Together, these traits make the Atacama Desert one of the harshest environments on Earth, which challenges life on many fronts and therefore is useful for determining the effects of Mars-like conditions on biology and the preservation and detection of life's organic building blocks.

The geological setting of the region is of considerable interest because of its value as an analog to certain martian surface environments and extreme conditions. Sulfate and chloride-rich deposits found on Mars have similar features

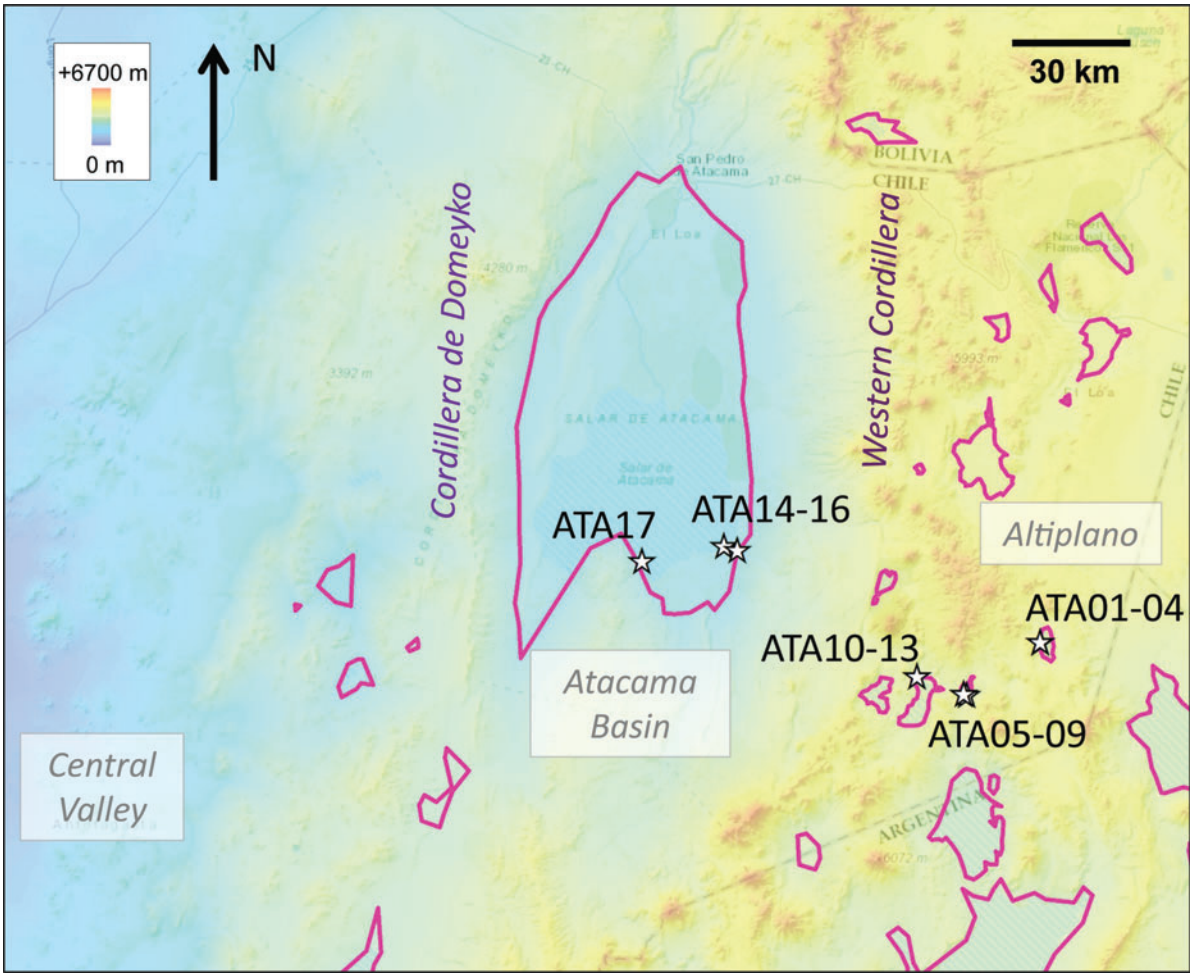

FIG. 1. Location of the study area within the Atacama Desert. ASTER GDEM is overlain in rainbow scale over the ArcGIS world topographic map (ArcGIS world imagery maps, ESRI/DigitalGlobe). The ASTER GDEM is a product of METI and NASA. Salars and sampling sites are indicated as magenta outlines and white stars, respectively. For Sample IDs and the names of their respective salars (Table 2). ASTER, Advanced Spaceborne Thermal Emission and Reflection Radiometer; GDEM, Global Digital Elevation Model. Color images are available online.

Downloaded by UPPSALA UNIVERSITETSBIBLIOTEK from www.liebertpub.com at 03/16/20. For personal use only.

Downloaded by UPPSALA UNIVERSITETSBIBLIOTEK from www.liebertpub.com at 03/16/20. For personal use only.

as those that are found in the salars of the Atacama Desert and may have formed via comparable processes (Sutter *et al.*, 2007; Flahaut *et al.*, 2017). The western section of the Atacama Desert lies over a sedimentary bedrock, the Andean section to the East, which encompasses our sampling area, and it is made of a variety of basaltic to dacitic volcanic rocks that may be similar to rocks of the martian crust (Flahaut *et al.*, 2017).

Still, current conditions on Mars are typified by extreme aridity, low temperatures (average −60°C), oxidizing surface conditions, and high radiation levels due to a thin atmosphere (Pavlov *et al.*, 2002; Quinn *et al.*, 2013; Hassler *et al.*, 2014), all of which are much more severe than in the Atacama Desert. These kinds of conditions would generally challenge the potential presence of carbon-based life, especially near the surface where radiation and oxidizing conditions are most extreme. However, evidence indicates that Mars had a more favorable climate (at least) during the first few hundred million years after its formation, including warmer temperatures and large bodies of liquid water (Pollack *et al.*, 1987; Squyres *et al.*, 2004; Poulet *et al.*, 2005; Bibring *et al.*, 2006; Mustard *et al.*, 2008; Ehlmann *et al.*, 2011). This evidence includes the detection of a multitude of (localized) hydrated minerals, including phylosillicates, sulfates, carbonates, and chlorides, which generally only form in aqueous environments (Gendrin *et al.*, 2005; Poulet *et al.*, 2005; Bibring *et al.*, 2006; Osterloo *et al.*, 2008; Murchie *et al.*, 2009).

Overall, there appears to be a widespread presence of water-lain sedimentary rocks, believed to have formed in shallow seas, lakes, and salars (Carr and Head, 2010; Hynek *et al.*, 2010; Grotzinger *et al.*, 2014; Flahaut *et al.*, 2015). Further evidence includes observations of a large number of apparent ancient river channels and valleys, which also strongly suggest that the flow of large bodies of water was once prevalent here (Carr, 1996; Carr and Head, 2010). However, it is believed that a climatic shift of planetary scale transformed Mars into the hostile planet we know today.

An additional interesting feature of the Atacama Desert is that it has also undergone a shift from wetter conditions in the past, to the current extreme aridity. Studies on the lithology of the region have described different depositional environments from the late Triassic up until today, which were summarized by Clarke (2006). Depositional environments during the Triassic include fluvial landforms overlain by marine sediments and alluvial fans, whereas the early Jurassic and Cretaceous are typified by marine to evaporitic marine environments and coastal saline lagoons, respectively. During the late Creataceous-Paleocene, westerly derived alluvial fans fed waters into playa lakes. At the time of the Oligocene-Middle Miocene, the region was overlain by a continental evaporitic lake that gradually changed into a continental playa lake toward the Plio-Pleistocene. Today, the region is typified by extreme aridity with scattered evaporitic lakes. This shift is largely recorded in the local bedrock and could also provide insight into processes that may have taken place on Mars as well.

The goal of this study is to investigate several of the salars in the Atacama Desert region with regard to their biological fingerprints. The driest parts of the Atacama region have long been believed to be devoid of life (Navarro-Gonzalez *et al.*, 2003). However, research efforts over the past 15 years have shown that even in the driest regions of the desert, microbial communities exist that have found ways to survive and even thrive under these extreme conditions, sometimes with a patchy distribution (Warren-Rhodes *et al.*, 2006; Lester *et al.*, 2007; Parro *et al.*, 2011; Patzelt *et al.*, 2014). Further, organic carbon has been shown to be present only in low abundances, which forces another limitation on the sustainment of microbial life in the region (Azua-Bustos *et al.*, 2017). We survey here the distribution of biological fingerprints at distinct locations that show different rock composition, elevation, temperatures, and proximity to water ponds.

A recent study by *Flahaut et al.* (2017) has focused in great detail on the mineralogy and geological settings of several salars in the Atacama Desert by using space-born, field (visible and near infrared [VNIR] spectroscopy), and laboratory-based analysis. During fieldwork, samples for biological analysis were collected and analyzed in the study presented here. The four salars that were investigated during this study were all located within the Antafogasta region of Northern Chile (Fig. 1). These salars include the Salar de Atacama, the largest of the salars, which is located on sedimentary basement and formed at intermediate elevations (2500 m) under hot and dry conditions. The other three salars investigated in this study are situated in the volcanic Andean highlands, at higher elevations (4000 m) and with slightly wetter and cooler conditions. For more details on the geological setting and mineralogical content of these salars, we refer the reader to the work of *Flahaut et al.* (2017).

Using Illumina 16S amplicon sequencing techniques, we found versatile microbial communities present within the investigated salars to be dominated by (extremely) halophilic organisms. Amino acids, organic carbon, and nitrogen were also identified, and our results indicate that the investigated salars can be considered bastions of life in one of the harshest environments on Earth. Therefore, areas on Mars showing similar features as the salars investigated in this study could be interesting targets for life detection missions on the Red Planet.

2. Materials and Methods

2.1. Sampling sites description

The sample material investigated in this study was collected from the Andean highlands (altitude of about 4500 m) and intermediate elevation sites (altitude up to 3000 m) of the Atacama Desert, Chile. Four different salars (Salar de Laco, Laguna Tuyajto, Salar de Aguas Calientes 3, and Salar de Atacama) were sampled at their center and margins during a field expedition led by the VU University of Amsterdam in March 2015 (Fig. 1). Samples of salt crusts and/or wet sediments were collected at both the surface and shallow depths (20–30 cm), when possible (Fig. 2). In Tables 1 and 2, a short description and GPS coordinates (Decimal Degrees) of the field sites and additional information of the sample material, including, for example, the number of samples collected at each field site, can be found. Figure 1 shows the specific locations at which sample material was collected. A detailed discussion of the field sites and the mineralogy of the investigated material can be found in the work of Flahaut *et al.* (2017).

FIG. 2. The different collections sites are shown and numbered according to their Location ID **(A–J)** (Table 2). Further information is listed in Tables 1 and 2. Color images are available online.

2.2. Sample preparation and methods

2.2.1. Amino acid extraction. The amino acid extraction procedure is briefly explained next. Detailed information can be found in the work of Botta *et al.* (2002). For sterilization purposes, all glassware and the columns with glass wool were double wrapped in aluminum foil and placed into a furnace at 500°C for a minimum of 3 h. Serpentine powder was sterilized as well at this temperature and used as an internal control to track potential contamination during the extraction procedure. Rock and sediment samples were dried in a centrifuge-dryer system (CentriVap Centrifugal concentrator/ColdTrap system, LabConco) before grinding them to fine powder in ceramic mortars with pestles in

Downloaded by UPPSALA UNIVERSITETSBIBLIOTEK from www.liebertpub.com at 03/16/20. For personal use only.

Table 1. General Description of the Four Different Salars Investigated During This Study

Salar	*Brine type*	*Mean elevation (m)*	*Mean Temp. (°C)*	*Evaporation (mm/year)*	*Area salar (km^2)*	*Main minerals detections (>50%)*
Salar de Aguas Calientes 3	Mixed	3950	1	1500	46	Gypsum, halite
Laguna Tuyajto	SO_4	4010	1	1500	2.9	Halite, gypsum, anorthite (detritic)
Salar de Laco	SO_4	4250	1	1500	16.2	Gyspum, carbonates, anorthite (detritic)
Salar de Atacama	Mixed	2300	14	1800	3000	Halite

Information on the different Salars was obtained from Flahaut *et al.* (2017).

a laminar flow. A total of 200 mg of powder material of each sample was transferred into glass tubes, and 3 mL of Ultra-High-Performance-Liquid-Chromatography/Mass Spectrometry (ULC/MS) pure grade water was added. The glass tubes were subsequently flame-sealed and placed into a heating box at the set temperature of 100°C for the next 24 h.

Subsequent to heating, the tubes were opened and centrifuged at 2500 rpm for 10 min to separate the supernatant from the solid part (total volume of supernatant 3 mL). Half of the supernatant (1.5 mL) was placed in 5 mL glass test tubes (labeled as H, for hydrolysis). The other half of supernatant was supplemented with 1 mL of ULC/MS pure grade water, vortexed, and centrifuged again at 2500 rpm for 10 min, after which all of the 2.5 mL of the supernatant was transferred into 5 mL glass tubes and labeled as NON-H (not hydrolyzed). All the samples were subsequently dried within the CentriVap/Coldtrap system. After drying, the glass tubes with the samples labeled as H (3 mL) were placed inside bigger glass tubes (20 mL) with 6 *M* HCl at the bottom, flame-sealed again, and placed into an oven at 150°C for 3 h to undergo acid hydrolysis. Afterward, these tubes were dried for 1 h by the CentriVap/Coldtrap system.

A total of 3–4 mL of a resin solution (100 mL ULC/MS pure grade water +24 mg of AG®50W-X8 Resin, Analytical grade 100–200 mesh purchased from Bio-Rad) was subsequently added to the columns with glass wool. A sequential

Table 2. Field Description of the Various Sampling Locations in the Four Different Salars That Were Investigated

SampleID	*Location ID*	*Reference*	*Location*	*Coordinates*	*Sample depth (cm)*	*Temp. at sample depth (°C)*
ATA01	A	J2L1R1Z1	Salar Laco, center	−23.84926°, −67.42459°	Surface	30.0
ATA02	A	J2L1R1Z2	Salar Laco, center	−23.84926°, −67.42459°	17–20	19.3
ATA03	B	J2L1R2Z1	Salar Laco, margin	−23.84876°, −67.42517°	Surface	29.5
ATA04	B	J2L1R2Z2	Salar Laco, margin	−23.84876°, −67.42517°	20	17.1
ATA05	C	J2L2R2S4Z1	Laguna Tuyajto, margin, close to water	−23.95548°, −67.58775°	Surface	25.4
ATA06	C	J2L2R2S6Z1	Laguna Tuyajto, margin, close to water	−23.95548°, −67.58775°	Surface	23.8
ATA07	D	J2L2R3S1Z1	Laguna Tuyajto, center	−23.95332°, −67.59512°	Surface	27.6
ATA08	D	J2L2R3S1Z2	Laguna Tuyajto, center	−23.95332°, −67.59512°	12	16.4
ATA09	E	J2L2R4Z2	Laguna Tuyajto, margin	−23.95965°, −67.59531°	12	19.4
ATA10	F	J5L1R3Z1	Salar Aguas Calientes 3, center	−23.91839°, −67.69846°	Surface	22.5
ATA11	F	J5L1R3Z2	Salar Aguas Calientes 3, center	−23.91839°, −67.69846°	8	16.1
ATA12	G	J5L1R4Z1	Salar Aguas Calientes 3, margin	−23.91834°, −67.69817°	Surface	23.0
ATA13	G	J5L1R4Z2	Salar Aguas Calientes 3, margin	−23.91834°, −67.69817°	24	11.5
ATA14	I	J7L14	Salar de Atacama (Peine Road), margin	−23.65346°, −68.12642°	Surface	48.2
ATA15	J	J7L16Z1	Salar de Atacama (Peine Road), margin	−23.66163°, −68.09688°	Surface	44.9
ATA16	J	J7L16Z2	Salar de Atacama (Peine Road), margin	−23.66163°, −68.09688°	15	29.4
ATA17	H	J7L9Z1	Salar de Atacama (Peine Road), center	−23.68421°, −68.30838°	Surface	43.0

Samples were collected either at the center of the salar or more toward its margins. The reference sample string was taken from Flahaut *et al.* (2017).

Downloaded by UPPSALA UNIVERSITETSBIBLIOTEK from www.liebertpub.com at 03/16/20. For personal use only.

Downloaded by UPPSALA UNIVERSITETSBIBLIOTEK from www.liebertpub.com at 03/16/20. For personal use only.

washing with basic-neutral-acid-basic solutions was made to activate the resin active sites. The basic solution (up to pH of 14) was a 2 *M* sodium hydroxide solution (8 g of NaOH in 100 mL of ULC/MS pure grade water), and the acid solution was a 1.5 *M* HCl acid solution (12.5 mL HCl in 87.5 mL of ULC/MS grade water). ULC/MS grade water was used for neutralization after basic and acid washing, until a pH of about 7 was reached.

After the sequential washing procedure, 3 mL of ULC/MS pure grade water was added to each dried sample and subsequently added to the column. The elution was collected and stored at about 4°C for further analysis. A total of 5 mL of a 2 *M* ammonia solution (ULC/MS grade water to 15.304 mL of 25% ammonia for a final volume of 100 mL) was added subsequently to the columns to remove the amino acids bound to the resin. The eluent was collected with glass tubes, and the ammonia was removed overnight by the CentriVap/Coldtrap system. The dried samples were either stored in a refridgerator or freezer or directly reconstituted in 100 μL ULC/MS grade water for subsequent analysis (see next sections).

2.2.2. Liquid chromatography mass spectrometry. An Agilent 1260 Liquid Chromatography-Mass Spectrometry (LC-MS) system equipped with a UV and fluorescence detector system, an autosampler module where the amino acid derivatization is performed, and a 500-MS ion trap mass spectrometer with electrospray ionization was used for amino acid analysis. The column used for analysis was a 150 × 3 mm 2.6 μm phenyl-hexyl stationary phase from Phenomenex, which was thermostatted at 25°C. The LC was operated in a binary gradient of mobile phases A (10 m*M* ammonium acetate in ULC/MS water) and B (ULC/MS grade methanol). The MS was operated in positive mode with optimized conditions for each individual amino acid.

Amino acids were derivatized by using a method based on the work of Nimura and Kinoshita (1986), which was then fully automated to increase the robustness of the method. This automation was achieved by programming the autosampler module (Agilent G1329B) of the LC-system to mix the various reagents. The approach used was as follows: The amino acid sample was diluted in a 1:1 ratio to yield a solution of amino acids in 0.1 *M* HCl and a set amount of internal standard (usually 100 m*M* norvaline). This was then mixed in a 1:3 ratio with 0.1 *M* sodium borate, and this mixture was then mixed in 2:1 ratio with methanolic o-phthaldialdehyde/N-acetyl-L-cysteine (OPA/NAC) (8 mg OPA and 10 mg NAC in 1 mL methanol), which was incubated for 2 min. Subsequently, 2.5 μL was injected into the system. In a typical measurement run, several samples were analyzed sequentially, including wash procedures and the analysis of amino acid standard solutions (part number: 5061-3332; Agilent). Amino acids were identified by comparison to retention times of known standards as well as their associated m/z ratio for the derivatized molecules. Standards were run in conjunction with sample analysis to track reagent degradation and system performance.

2.2.3. Gas chromatography mass spectrometry

2.2.3.1. Amino acid derivatization. A water extract (25 μL) was transferred into a reaction vial, the total volume was adjusted to 50 μL with 0.2 *M* HCl solution, and a 2,2,3,3,4,4,4-heptafluoro-1-butanol/pyridine mixture (3:1, *v/v*; total volume 25 mL), followed by 5 μL of ethyl chloroformate, was added. The vials were capped tightly and shaken vigorously for 10 s to form N-ethoxycarbonyl heptafluorobutyl ester (ECHFBE) derivatives. Finally, the ECHFBE derivatives of amino acids were extracted into the organic phase from the reactive mixture by adding 50 μL of methyl laurate in chloroform (10^{-5} *M*), and the latter served as an internal standard. The organic phases were withdrawn and transferred into 1 mL GC vials equipped with 100 μL inserts for enantioselective Multidimensional Gas Chromatography (GC × GC) analyses.

2.2.3.2. Multidimensional gas chromatography mass spectrometry. The enantioselective multidimensional analysis was carried out by GC × GC Pegasus IV D coupled to a time-of-flight mass spectrometer (LECO, MI). The mass spectrometric system operated at a storage rate of 150 Hz, with a 50–400 amu mass range, detector voltage of 1.8 kV, and solvent delay of 15 min. The ion source and injector temperature were set at 230°C. In all runs, the column set consisted of a Chirasil-L-Val column (24.885 m × 0.25 mm, 0.12 μm film thickness) in the first dimension and DB Wax as a secondary column (1.19 m × 0.1 mm, 0.1 μm film thickness) coupled to a modulator (0.21 m × 0.1 mm, 0.1 μm film thickness). The maximum operating temperatures of the columns were 200°C and 250°C, respectively. Helium was used as a carrier gas at a constant flow of 1 mL/min.

All samples were injected in the splitless mode by applying the identical temperature program. The temperature of the primary column was held at 40°C for 1 min, and then it was increased to 80°C at a rate of 10°C min^{-1} and held at this temperature for 5 min. Finally, the primary column was heated up to 180°C with 2°C min^{-1} rate and held at this point for 7 min. The secondary oven used a temperature offset of 30°C. It was held at 70°C for 1 min, warmed up to 110°C with 10°C min^{-1} rate, and held at this temperature for 5 min The oven was then heated up to 160°C at a rate of 2°C min^{-1}, finally increased to 220°C at a rate of 4°C min^{-1}, and held for 22 min. A modulation period of 5 s was applied. The derivatized soil and serpentine extracts, as well as corresponding replicates, were injected three times to ensure accuracy of calculated peak area with reliable statistical error bars. Data were processed with the LECO Corp ChromaTOF™ software. Volume peak integrations were performed, taking into account possible modulation-induced errors (Meinert and Meierhenrich, 2012).

2.2.4. Illumina 16S amplicon sequencing

2.2.4.1. DNA extraction. Rock and sediment samples were dried in an oven at 80°C overnight and subsequently powdered with a sterile mortar and pestle (DNA-away solution, heat sterilization, and UV sterilization). The DNeasy PowerSoil extraction kit (Qiagen, Hilden, Germany) was used for the DNA extraction of the samples. Because of an expected low biomass, an adapted protocol was used to minimize sorption of DNA by the mineral matrix (Direito *et al.*, 2012). Further, the DNA extract was eluted in 70 μL instead of the regular 100 μL to further increase the concentration of the extract. All handlings of the samples and negative controls during the extraction process

Downloaded by UPPSALA UNIVERSITETSBIBLIOTEK from www.liebertpub.com at 03/16/20. For personal use only.

were conducted in a UV3 HEPA PCR workstation (UVP, Upland, CA), equipped with a High-Efficiency-Particulate-Air (HEPA) filter and a UV illuminator to prevent extraneous DNA contamination. Concentrations of the extracts were determined with a Quant-iT high-sensitivity DNA assay kit and a Qubit® fluorometer (Invitrogen, Carlsbad). DNA extracts were stored at −20°C until further processing.

2.2.4.2. Illumina 16S amplicon sequencing. All DNA extracts were diluted to a concentration of 0.1 ng/μL before polymerase chain reaction (PCR) amplification. If the concentration of the DNA extract was lower than 0.1 ng/μL, it was processed undiluted. PCR reactions were performed in triplicate by using Phusion Green Hot Start II High-Fidelity DNA Polymerase (Thermo Fisher Scientific, Sweden). We targeted the V3–V4 region of the 16S rRNA gene, using the V3 forward primer S-D-Bact-0341-b-S-17, 5′-CCTACGGG NGGCWGCAG-3′ (Herlemann *et al.*, 2011) and the V4 reverse primer S-D-Bact-0785- a-A-21, 5′-GACTACHV GGGTATCTAATCC-3′ (Muyzer *et al.*, 1993), giving rise to ∼430 bp long double-stranded DNA fragments. The primers were dual barcoded and compatible with Illumina sequencing platforms as previously described (Caporaso *et al.*, 2011).

Performance of the PCR reaction was checked by running incorporated positive and negative controls from each triplicate plate on 1.5% (w/v) agarose gels. Triplicate PCR products were combined, and each combined triplicate sample was purified by using SPRI beads (Agencourt® AMPure® XP, Beckman Coulter, CA). The DNA concentration in the purified samples was determined as described earlier. Samples were diluted to identical concentrations of 2 ng/μL before pooling the diluted PCR products together in equal volumes (10 μL) in one composite sample (including positive and negative controls).

The composite samples were paired-end sequenced at the Vrije Universiteit Amsterdam Medical Center (Amsterdam, The Netherlands) on a MiSeq Desktop Sequencer with a 600-cycle MiSeq Reagent Kit v3 (Illumina) according to the manufacturer's instructions. High-throughput sequencing raw data were demultiplexed with bcl2fastq software version 1.8.4 (Illumina), and primers were trimmed by using Cutadapt (Martin, 2011). Demultiplexed samples were further processed by using a modified version of the Brazilian Microbiome Project 16S profiling analysis pipeline (Pylro *et al.*, 2014). Paired-end reads were joined by using PANDAseq (Masella *et al.*, 2012), selecting for a minimum overlap of 30 nucleotides between the forward and reverse reads.

We selected for a minimum sequence length of 285 bp, and no mismatches in the primer region were allowed. PANDASeq addresses mismatches in overlapping regions by selecting the nucleotide with the best sequencer-assigned quality score. Because PANDAseq incorporates a base quality filter during read assembling, the threshold for consecutive high-quality bases per read was set to zero. Metadata and demultiplexed samples were merged by using add_qiime_labels.py (Caporaso *et al.*, 2010), and sequence headers were changed by using bmp-Qiime2Uparse.pl (Pylro *et al.*, 2014). UPARSE was used to dereplicate, filter chimeras, and discard operational taxonomic units (OTUs) detected less than two times and OTU clustering at 97% similarity (Edgar, 2010, 2013).

The OTU taxonomy was assigned by using the UCLUST algorithm (Edgar, 2010) on Quantitative Insights in Microbial Ecology (QIIME) (Caporaso *et al.*, 2010) with SILVA compatible taxonomy mapping files (Silva database release 128) (Quast *et al.*, 2013; Yilmaz *et al.*, 2014) and aligned with align_seqs. py in QIIME (Caporaso *et al.*, 2009). Taxonomy was manually curated and refined up to genus level based on 97% similarity of reference sequences. The reference tree was calculated by using the make_phylogeny script in QIIME (Price *et al.*, 2009). We generated a Biological Observation Matrix (BIOM) file by using make_otu_table.py on QIIME (Caporaso *et al.*, 2010). Before further analysis, we produced an OTU table and a taxonomy table with BIOM scripts (McDonald *et al.*, 2012).

The OTUs detected in negative controls and procedural blanks were manually removed from the dataset. After quality filtering, taxonomy assignment (97% identity), subtraction of contaminating sequences, and removal of singletons, the dataset comprised 731,249 reads, which were attributed to a total of 3900 OTUs. Next, a filtering step was performed as described by Bokulich *et al.* (2013), where OTUs representing fewer than 0.005% of the total reads were removed from the dataset. This trimmed dataset resulted in 700,874 reads and a total of 1404 OTUs. This dataset was rarefied by choosing 1000 reads as the minimum count to include 16 of the 17 samples, resulting in a dataset comprising 16,000 reads and 1135 OTUs.

2.2.5. Carbon and nitrogen measurements. Samples were powdered with a heat-sterilized mortar and pestle and subsequently dried at 60°C for 24 h. Analysis was carried out with a FlashEA 1112 (Thermo Scientific), with EAGER300 operating software and a thermal conductivity detector. For carbon and nitrogen measurements, ∼30 mg of each sample was weighed in silver holder cups. An empty holder cup was used as a blank. A total of 2–3 mg of Ethylenediaminetetraacetic acid was used as standard (7.522% N, 32.237% C, 4.836% H, 34.386%). For the removal of inorganic carbon, cups that contained the samples were placed upright in a desiccator containing 12 *M* HCl. Samples were exposed overnight to the vapors. Complete removal of inorganic carbon was tested by adding 10 μL of 10% HCl to a cup to determine whether vapors were produced (which would indicate the presence of more inorganic carbon). This procedure was repeated until no further fumes were produced. Samples were dried at 80°C before Carbon-Nitrogen (CN) measurements. The silver cups were sealed off and placed within a tin cup, which was sealed before measurement. Abundances were measured as percentage per weight, and measurements were carried out in duplicate.

3. Results

In this section, we show the biological fingerprints obtained from the different rock and sediment samples from the four different salars. By combining the results obtained from different measurement techniques and taking into account the environmental differences between the sampling sites, we aim at creating an overview of microbial life and its subsequent building blocks, which thrives in these types of salars, and how this is relevant for the search for life on Mars.

Downloaded by UPPSALA UNIVERSITETSBIBLIOTEK from www.liebertpub.com at 03/16/20. For personal use only.

3.1. LC-MS and GC×GC-MS analysis of amino acids

Amino acids were measured to obtain a general overview about the biological load in the soil samples. The soil samples were divided into two different sets (ATA01-ATA09 and ATA10-ATA17), and these sets were analyzed by different measurement techniques (LC-MS and Multidimensional Gas Chromatography Mass Spectrometry [GC×GC-MS], respectively). Due to the use of different techniques and standards, some amino acids were not measured for both sample sets, and the D-amino acids were only determined by GC×GC-MS. Therefore, we will mainly focus on the amino acids that were determined by both measurement techniques. Amino acids are considered high priority targets in the search for extraterrestrial life since they make up the building blocks of the entire protein machinery of life on Earth but are also commonly found in meteorites (Ehrenfreund and Charnley, 2000; Martins *et al.*, 2008; Aerts *et al.*, 2016), indicating that these building blocks of life are common organic compounds in our Solar System.

Amino acids were detected in readily detectable quantities in most samples, in highly variable amounts (Table 3). A few samples have considerably lower abundances of amino acids. These include one sample collected from the drier central part of Laguna Tuyajto (ATA08) and two samples from Salar de Atacama (ATA15 and ATA17). These amino acid values are more similar to those of samples obtained from the driest region in the Atacama Desert (Yungay), which were previously analyzed (Skelley *et al.*, 2005; Amashukeli *et al.*, 2007). However, overall, we detected relatively high concentrations of amino acids in comparison to other regions in the Atacama Desert, and this is likely linked to the presence of surface water and/or a more pronounced presence of life that is found in the Andean altiplano. Further, proteinogenic amino acids are by far the most abundant types we found, and enantiomeric

Table 3. Amino Acids Identified and Quantified in Atacama Samples Using LC-MS and GC×GC-MS

Compound	*ATA01*	*ATA02*	*ATA03*	*ATA04*	*ATA05*	*ATA06*	*ATA07*	*ATA08*	*ATA09*
				LC-MS measurements					
L-*Asp*	BB	4.6636	39.6980	45.4882	22.8467	n.a.	15.9786	BB	20.4145
L-*Glu*	40.8835	16.6413	139.3258	133.2587	71.6233	n.a.	38.5571	LOQ	35.3504
L-*Ser*	14.8565	10.5807	34.7016	32.0143	38.8338	n.a.	10.8616	1.6199	14.0343
L-*Thr*	8.2926	7.2422	35.2993	39.4337	22.2787	n.a.	20.1369	1.5384	24.4815
Gly	28.4561	29.2985	112.5927	130.3262	184.0706	n.a.	32.5197	19.7174	76.5153
β-Ala	2.7706	1.7261	10.0720	14.5592	26.9636	n.a.	1.8149	2.2183	7.1848
L-*Ala*	14.8567	9.4829	52.6682	60.9958	83.4233	n.a.	27.5205	5.5068	41.2645
L-*Lys*	26.9343	179.6670	183.3782	6.3372	92.4194	n.a.	BB	BB	61.9660
L-*Val*	3.5567	25.3343	28.0825	12.5779	21.5742	n.a.	54.8623	1.9426	27.5493
L-*Met*	70.8579	64.3128	BB	1.0020	BD	n.a.	BD	6.0634	BD
L-*Iso-Leu*	30.1724	LOQ	22.8995	21.2417	BB	n.a.	27.8112	BB	28.4878
L-*Phe*	153.4099	294.5115	257.4771	90.9713	7.3644	n.a.	18.1102	1.2591	23.0885
L-*Leu*	25.4313	40.9702	70.5916	49.6273	27.4641	n.a.	BB	22.0848	12.0110

Compound	*ATA10*	*ATA11*	*ATA12*	*ATA13*	*ATA14*	*ATA15*	*ATA16*	*ATA17*
				GC×GC-MS measurements				
Gly	1370±40	1330±60	240±20	140±11	BB	185±16	195±8	BB
D-*Ala*	39±4	39±4	LOQ	BB	BB	LOQ	3.12±0.19	BB
L-*Ala*	510±30	510±30	74±6	46±2	BB	136±6	48±4	BB
β-Ala	28±3	27±2	11.6±1.9	BB	BB	BD	9±1	BD
D-*Ser*	1.39±0.17	1.39±0.17	BD	BD	BD	BD	BD	BD
L-*Ser*	5.0±0.5	5.0±0.5	LOQ	LOQ	BD	BD	LOQ	BD
D-*Asp*	211±14	211±14	17.1±1.8	15.1±0.3	LOQ	1.3±0.13	18.4±0.7	BD
L-*Asp*	610±60	900±60	73±7	66.3±0.9	4.3±0.4	4.0±0.4	126±8	BD
D-*Val*	8.2±0.4	8.0±0.5	1.47±0.13	0.75±0.07	LOQ	3.23±0.05	0.97±0.04	BD
L-*Val*	310±20	290±20	51±5	30.7±1.2	5.65±0.84	179±17	39±4	BB
D, L-*Pro*	120±12	134±3	27.7±1.6	9.2±0.8	1.42±0.14	37.6±1.1	24.9±1.1	BB
D-*Glu*	56±4	76±4	20±2	10±2	BD	BD	24±2	BD
L-*Glu*	620±40	620±40	174±8	78±9	LOQ	19.5±1.6	127±8	BD
D-*Iso-Leu*	5.0±0.3	4.9±0.3	0.65±0.05	0.40±0.04	LOQ	2.44±0.12	LOQ	BD
L-*Iso-Leu*	159±14	159±14	20±2	14.1±0.8	3.7±0.2	96±9	20.7±1.6	BB
D-*Leu*	7.7±0.5	7.7±0.5	0.77±0.06	0.56±0.07	LOQ	3.7±0.3	0.85±0.06	BD
L-*Leu*	237±16	237±17	25±2	19.8±1.1	1.69±0.2	113±8	26.1±1.8	BB
D-*Phe*	7.0±0.5	7.0±0.5	0.44±0.08	0.60±0.08	BD	0.87±0.06	LOQ	BD
L-*Phe*	141±9	141±9	9.7±0.7	13.8±0.4	1.11±0.08	33±3	14.7±1.2	BD

Abundances are given in (nanomol/gram soil); LC-MS: for displayed values a measurement uncertainty of 10% is applied; GC×GC-MS: displayed values with a confidence interval of 3σ. Only the most abundant amino acids are shown in the table.

BB, below blank; BD, below detection sensitivity; GC×GC-MS, Multidimensional Gas Chromatography Mass Spectrometry; LC-MS, liquid chromatography/mass spectrometry; LOQ, limit of quantification; n.a., sample not measured.

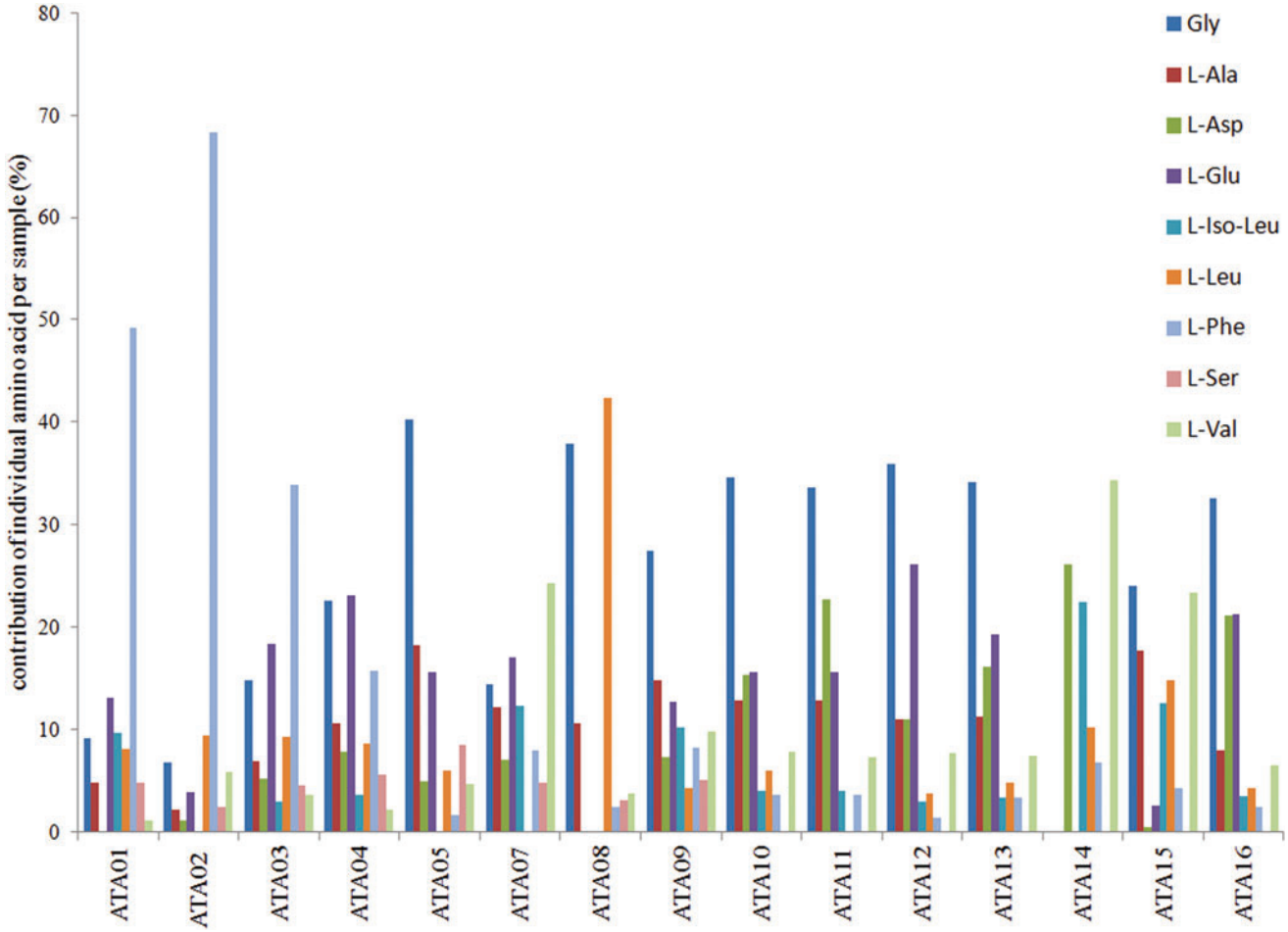

FIG. 3. Relative contribution of nine selected (most dominant) amino acids per investigated sample. ATA01–ATA04: Salar de Laco; ATA05–ATA09: Laguna Tuyajto; ATA10–ATA13: Salar de Aguas Calientes 3; ATA14–ATA16: Salar de Atacama (Peine road). ATA06 was not measured for amino acids and for ATA17 no amino acids were detected. Color images are available online.

ratios (L-amino acids have higher abundances than their D-amino acids counterparts) clearly indicate biotic origin of these molecules (Meierhenrich, 2008). An overview of the relative contribution of the most dominant L-amino acids in each sample is shown in Fig. 3.

Samples collected from Salar de Laco (ATA01–ATA04) all showed similar abundances of total amino acids, whether they were collected at the margin or at the center of the salar. Both locations showed a similar composition with a high proportion of dentritic material. Distributions of the individual amino acids differ somewhat (*i.e.*, Glycine is much more dominant in ATA03 and ATA04, whereas Methionine is abundant in ATA01 and ATA02 but virtually absent in the other two samples), but overall most amino acids are present in a similar order of magnitude.

Samples from Laguna Tuyajto showed some more pronounced differences between the sampling locations in terms of total amino acid content. ATA05, which was taken at the external margin of the salar and close to the water body, revealed the highest total amino acid abundances. During DNA extraction, this sample was also observed to have a high DNA load (Fig. 4). ATA07 and ATA08 were sampled at the center of the salar with no nearby presence of water and were composed of pure salts. These samples

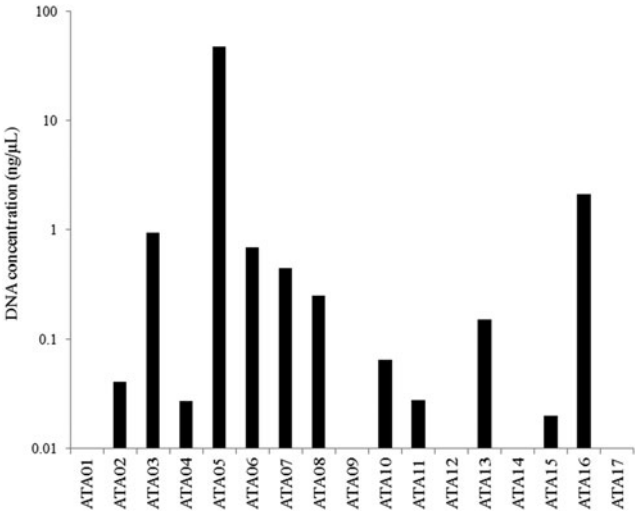

FIG. 4. DNA concentration in the extracts of the analyzed soil samples shown in logarithmic scale. Several samples were shown to have DNA load below our initial detection limit, but all except one (ATA14) revealed the presence of enough genomic material for analysis after polymerase chain reaction amplification.

Downloaded by UPPSALA UNIVERSITETSBIBLIOTEK from www.liebertpub.com at 03/16/20. For personal use only.

Downloaded by UPPSALA UNIVERSITETSBIBLIOTEK from www.liebertpub.com at 03/16/20. For personal use only.

showed lower abundances of amino acids, whereas ATA09 (sampled between the external margin and the center) had amino acid abundances in the range somewhere in the middle between the other two sample locations in this salar.

Samples ATA10 and ATA11 from Salar Aguas Calientes 3 had by far the highest total load of amino acids of all the samples analyzed (5–10 × higher than other samples with significant amino acid concentrations). These samples were collected on a pebble beach section close to a water body, which may explain the increased abundances. Organic materials dissolved in the water are likely to seep into the surrounding soils or may have left behind organic molecules during a time of higher standing water. Samples ATA12 and ATA13, taken closer to the center portion of the same salar, had much lower abundances of amino acids.

Very low concentrations of amino acids were found in sample ATA14 from Salar de Atacama. This sample was also excluded from the DNA sequence analysis due to a lack of sufficient amplifiable genomic material in the DNA extract. ATA17, another sample from the same salar, with a thick and dry halite core, did not reveal the presence of amino acids above the detection limit. This sample also contained no detectable DNA in the original extract; however, after PCR amplification, enough material was found for sequence analysis. ATA15 and ATA16 had the highest amino acid loads of samples from Salar de Atacama. These sampling sites had significant vegetation, which may explain higher amino acid abundances. In both samples, genomic material was detected in the original extract.

3.2. Microbial community analysis

DNA was extracted from the soil samples to determine the composition of microbial communities present within the soil samples by using Illumina 16S amplicon sequencing. The main goal of DNA analysis was to determine which type of microorganisms are present in environments such as these. DNA quantities in the soil were overall low, but in the majority of the samples detectable DNA was present (Fig. 4); whereas in some samples, DNA load was rather high (notably ATA05, of which the analyzed sediment had a greenish color). This suggests that in most of the investigated soils, microbes (or plant life) are present in easily detectable numbers without the need for amplification techniques. Further, surface and subsurface samples were taken at most sampling sites (Table 2), and although it would generally be expected that subsurface samples would result in the recovery of lower biomass due to the absence of photosynthetic processes, there was no such trend observed here. This is likely due to the low depth from which samples were acquired (10–25 cm), and it may not be very representative for future Mars missions (*i.e.*, ExoMars) that aim at drilling to a depth of 2 m for sample collection (Vago *et al.*, 2017). However, due to strong UV radiation and high evaporation rates at the surface in this specific region, microbial life may endure better at depth.

Sequencing results reveal the presence of diverse prokaryotic communities, and a total of 1404 OTUs were found after removal of contaminating sequences and filtering steps. The dataset was rarefied (*i.e.*, the same number of sequence reads were picked from each sample at random) to create equal library sizes for the samples in downstream analysis so that samples could be compared in terms of relative abundances of the different putative species present. Generally, rarefaction resulted in dismissing only the least abundant OTUs from the dataset. The number of OTUs per sample shows that there is quite some diversity in the number of species, whether they came from the same area or from different sampling sites (Fig. 5).

The composition of the microbial community in each sample is shown at the phylum level in Fig. 6. Members of the extremely halophilic archaeal family *Halobacteriaceae* (Phylum *Euryarchaeota)* dominate the dataset at family level, making up for 39% of the total number of sequence

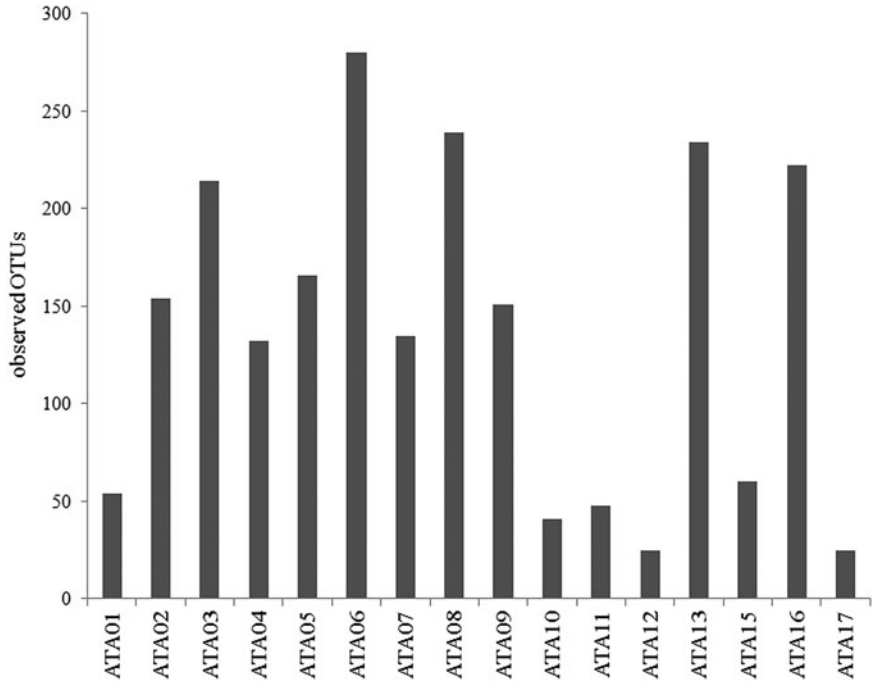

FIG. 5. Observed OTUs per sequenced soil sample in the rarefied dataset. OTUs, operational taxonomic units.

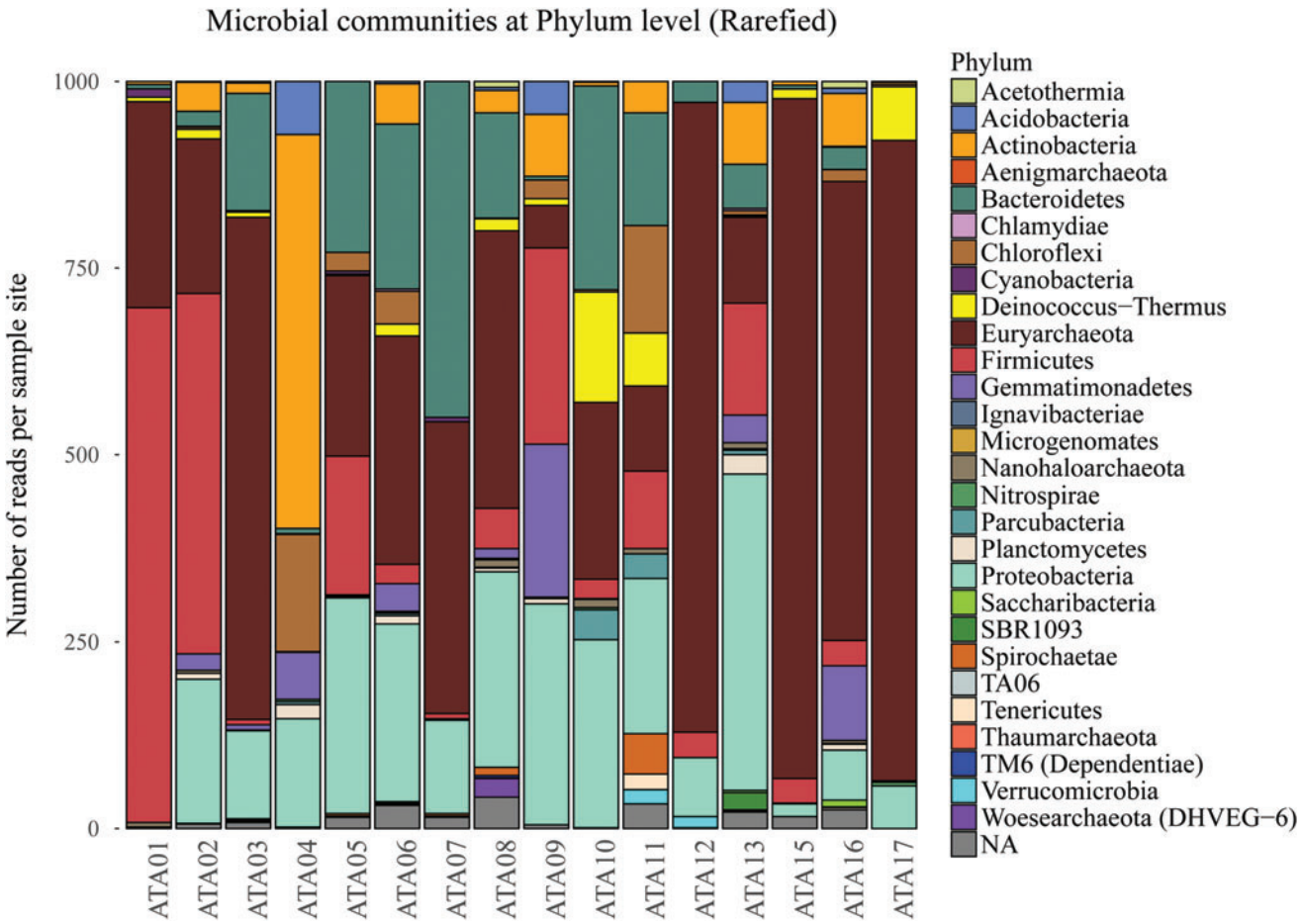

FIG. 6. Stacked barplot depicting the microbial diversity in the soil samples at Phylum level according to the rarefied 16S amplicon sequencing dataset. Color images are available online.

Downloaded by UPPSALA UNIVERSITETSBIBLIOTEK from www.liebertpub.com at 03/16/20. For personal use only.

reads. Some of the most dominant genera from this family are: *Haloparvum*, *Natronomonas*, *Halorubrum*, *Halomicrobium*, and *Haloarcula*. However, a total of 36 different genera of this family were present within the dataset. The *Halobacteriaceae* family members are present in higher numbers in the samples in which higher temperatures were measured and are also extremely dominant in the three analyzed samples taken from Salar de Atacama and one surface sample of Salar de Aguas Calientes 3 (ATA12), which was described as having a pinkish mud surface (the pink color likely hails from the distinct carotenoids that members of the *Halobacteriaceae* family produce). Together with the *Euryarchaeota*, the phyla *Proteobacteria* (18%), *Firmicutes* (13%), and *Bacteriodetes* (11%) contribute to about 80% of all the OTUs in the dataset.

Another extremely halophillic microorganism present in relatively high abundance was a bacteria of the genus *Salinibacter* (*Bacteriodetes*), which makes up almost 5% of the total number of reads. This species was found predominantly in the surface samples and not significantly in samples taken at increased depth. The most dominant genus found in the dataset was a *Bacillus* (*Firmicutes*) species (9%), which is likely a sporeformer, which allows it to survive harsh conditions for extended periods. This species was present in most of the samples but was exceptionally prominent in two samples of the central part of the Salar Laco (ATA01 and ATA02). At the center, the salt crust is dominated by gypsum and is generally thicker and drier than at its margins, where detritic components such as anorthite and water are more prominent (Flahaut *et al.*, 2017). Generally, the extraction of DNA from sporulated microorganisms is inefficient due to their resistance to extraction techniques. Therefore, finding such high numbers of a *Bacillus* species in the dataset could indicate that they are either in an active nonsporulated state or even more abundant in the microbial communities and only a fraction of their DNA was extracted.

Another prominent species found in the dataset is an uncultured member of the *Ectothiorhodospiraceae* (*Proteobacteria*) family, part of the purple sulfur bacteria. These organisms are capable of photosynthesis and mostly oxidize sulfite or thiosulfate under anoxic or microoxic conditions to elemental sulfur. These types of organisms are usually found in permanently stratified (often saline) lake environments such as the salars investigated here (Hunter *et al.*, 2008). Further, an uncultured species of the order of *Acidimicrobiales* (*Actinobacteria*) makes up 3% of the total number of reads (mainly due to the high presence in one sample), and several species of extremophiles belonging to the Phylum *Deinococcus-thermus* make up another 2.5% of the total number of reads.

It is interesting to note that one sample taken from the subsurface (ATA04) has no contribution at all from members of the *Halobacteriaceae* family and appears to have a very different microbial composition, which is dominated by

an uncultured member of the *Acidomicrobiales* order. Other dominant species in this sample are from the phyla *Chloroflexi*, more *Actinobacteria*, and a *Marinobacter* species. Most dominant species in this specific sample are only present (if present at all) in low abundances in the other investigated soil samples, making this particular sample rather unique.

This is also observed in the principle component analysis plot in Fig. 7 where ATA04 is strongly separated from all other samples based on its species composition. The sediment sample was taken at 20 cm depth from a compact pure calcite crust that was covered by two distinct clay layers. Flahaut *et al.* (2017) proposed that Salar de Laco used to be a lake with possibly alkaline waters that progressively dried out and became more acidic. This was found to be consistent with previously reported aerial imagery that identified ancient shorelines in this area. Patchy distribution of sedimentary features of this ancient environment in the subsurface could explain why the microbial composition of this particular sample, but not all samples from Salar de Laco, was so affected.

To determine whether the salars harbor distinctively different microbial communities, principle coordinates analysis was performed (Fig. 7). Some cluster formation is observed for the different salars; however, there is also considerable overlap and sometimes samples (*i.e.*, microbial communities from different salars are more similar than samples from the same salar). The three Salar de Atacama samples (Peine Road) form a more pronounced separate cluster as compared with the bulk of the other samples, suggesting that local conditions in this salar affect the microbial composition of the communities. However, samples from Salar de Laco and Salar de Aguas Calientes 3 also group within this cluster, and all have very high contributions of Halobacteriaceae species. Using Adonis tests, we found that sampling location (*i.e.*, the salar from which the sample was taken) ($p = 0.028$; $R^2 = 0.4$), sampling depth ($p = 0.015$; $R^2 = 0.21$), and the soil temperature ($p = 0.002$; $R^2 = 0.47$) had significant effects on the variation and abundances observed within the samples' microbial communities. Effect sizes (R^2) quantify the amount of variation explained by the chosen parameter (*i.e.*, sample location, sampling depth, soil temperature) in its respective ordination.

So, in their respective ordinations we find that 40% of the observed variation can be explained by sampling location, 21% by sampling depth, and 47% by soil temperature. However, the combined effects of these three measured variables (and likely more hidden variables) result in an image that suggests that regional, as well as local and small-scale factors influence distribution of microbial communities. No significant effect was found when looking at whether the

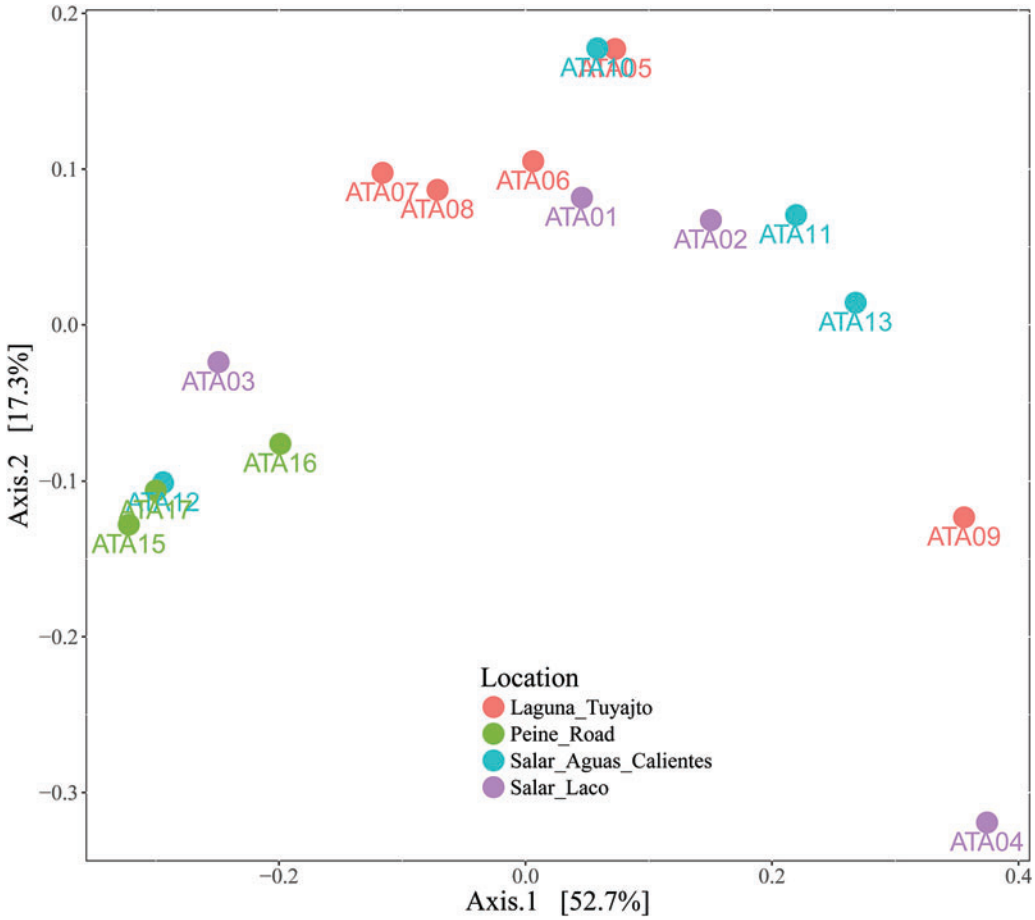

FIG. 7. Principle coordinates analysis plot using weighted unifrac metrics visualizing the beta diversity (how different the samples are in terms of species composition and relative contribution) of the microbial communities at the OTU level present in the samples from the different salars. Individual samples are colored according to their respective salars. Color images are available online.

Downloaded by UPPSALA UNIVERSITETSBIBLIOTEK from www.liebertpub.com at 03/16/20. For personal use only.

sample was taken at the (often wetter) margin or the center of the salar. In the accompanying paper focusing on the mineralogy of these salars (Flahaut *et al.*, 2017), it was found that different mineralogy dominates at the center of the salars (salts) if compared with the margins (more detrital material, carbonates, and clays). This does not appear to significantly affect the composition of the microbial communities on its own and is likely linked to the mixed nature of many of the sediments. In general, the species distributions of the different samples did not follow distributions in the quantitative presence of halite or gypsum that were determined for the sediments by Flahaut *et al.* (2017).

3.3. Organic carbon and nitrogen content

Overall, low concentrations of organic carbon and nitrogen were measured (Fig. 8), with carbon measurements typically (far) below 0.5 weight percentage and nitrogen load an order of magnitude lower (resulting in C/N ratios varying between 8 and 14). Especially samples ATA01, ATA02, ATA12, ATA14, and ATA17 have extremely low carbon (0.05–0.11% weight) and are comparable to soils from the most arid region in the Atacama Desert (Yungay) in terms of their organic carbon load (Lester *et al.*, 2007). In four of these five extremely low carbon samples, also no measurable DNA (below detection limit) was detected in the original extract before PCR amplification. There was only one other sample that contained no detectable DNA (ATA09, which also had fairly low carbon: 0.19%). Further, ATA05 and ATA06, having significantly higher carbon than the other samples, were sampled at the margin of their respective salar and were relatively close to a water body. The presence of water may partially explain their higher carbon and nitrogen content, which correlates with the presence of more pronounced life. This is also observed in the DNA extracts where especially ATA05 and, to a lesser degree, ATA06 show relatively high concentrations of DNA.

4. Discussion

The amino acids that were detected in high abundances in the investigated soil samples all fall in the category of most dominant amino acids in the protein machinery of the three kingdoms of Archaea, Bacteria, and Eukarya (Kozlowski, 2016). Further, a recent report by NASA, regarding the lander mission on Jupiter's moon Europa (Hand *et al.*, 2017), specifies seven amino acids (Ala, Gly, Leu, Ser, Val, Asp, Glu) as important ''biomarkers'' due to their relatively high abundance in biological systems on Earth as well as in extraterrestrial samples such as carbonaceous meteorites, which suggests that these molecules are widely spread throughout our Solar System. All seven of these amino acids were detected in relatively high quantities in these samples.

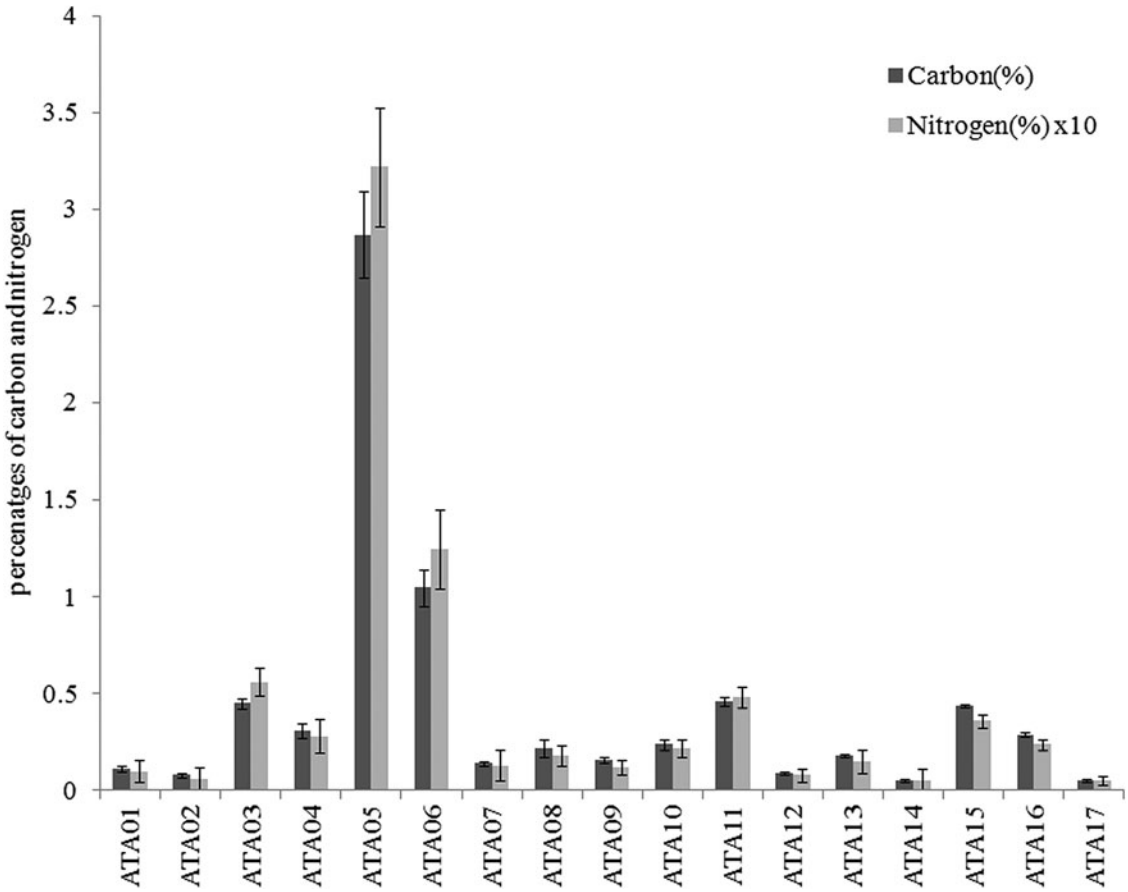

FIG. 8. Organic carbon and nitrogen load in the soil samples shown in weight percentages. Nitrogen values are enhanced by a factor 10 in this figure for clarity and visualization. Measurements were performed in duplicate, and standard deviations of the mean are shown.

Downloaded by UPPSALA UNIVERSITETSBIBLIOTEK from www.liebertpub.com at 03/16/20. For personal use only.

Downloaded by UPPSALA UNIVERSITETSBIBLIOTEK from www.liebertpub.com at 03/16/20. For personal use only.

In conjunction with these seven amino acids, we also detected Phenylalanine and Iso-Leucine in high quantities with strong enantiomeric excess of the L-isomer. Although less common in carbonaceous chondrites, these two amino acids could also be considered interesting biomarkers (as would be all proteinogenic amino acids) since their presence would point toward more complex (*i.e.*, biotic) synthesis processes. However, the presence of amino acids should clearly not be considered a signature of life on its own. Distribution patterns and enantiomeric excesses should also be considered.

When looking at the relative contribution of the nine most dominant L-amino acids per sample, some variation between samples can be observed (Fig. 3). Most notably, samples ATA08 and ATA14 deviate from the other samples. This is likely connected to the relatively low total amino acid load detected in these samples. Further, it is interesting to note that specifically samples from Salar de Laco have relatively high contributions of Phenylalanine, whereas this is mainly a minor contributor in samples from the other salars, where generally Glycine is the most dominant amino acid. Although there are marked differences in amino acid distribution between the different samples, ''fingerprints'' as observed here can serve as strong biomarkers.

Even though there are differences, the general constitution of these samples does not appear random and a certain trend of dominant and less dominant amino acids is observed within most samples. Distributions of amino acids produced by abiotic processes differ significantly from distributions that arrive from biological systems, which is mainly caused by the importance of function in the latter as opposed to ''random'' thermodynamic processes that influence the formation of the former (Higgs and Pudritz, 2009). It may, therefore, be more fitting to focus on relative contribution within a sample, rather than focusing on the quantification of individual amino acids.

Higher initial concentration of DNA in the extracts did not *per se* result in a higher number of microbial species in the sample communities, although samples with the highest initial DNA load tend to have relatively high alpha diversity (*i.e.*, samples ATA05, ATA06, and ATA16). Sample ATA14 was excluded from the rarefied dataset, because there were not enough sequence reads to include it in the analysis (low biomass). This sample was collected at the Salar de Atacama, which is the driest and hottest region of the different sampling locations. Samples from Laguna Tuyajto showed the highest numbers of species within the soil, followed by samples from Salar de Laco; whereas samples from Salar de Atacama and from Salar de Agua Calientes 3 showed, on average, a significantly lower number of species. Laguna Tuyajto was shown by Flahaut *et al.* (2017) to have the highest mineral diversity of the four salars along its wet margins, which may be reflected in the alpha diversity we observe here. This salar as well as Salar de Laco were derived from SO_4-rich brines and showed generally the highest species diversity. Both Salar de Atacama and Salar de Aguas Calientes 3 were shown to have relatively thick halite crusts that were derived from mixed Ca/SO_4-rich brines and were shown to have lower average alpha diversity.

Overall, there appears to be potential for a wide mix of metabolisms based on the 16S data, which include a multitude of organisms that are capable of sulfur and nitrogen metabolism; photosynthesis; heterotrophic, autotrophic, and chemolithotrophic metabolism; and aerobic, anaerobic, or microaerobic respiration. This observation shows that even though these salars are considered extreme environments on their own, they are still capable of supplying the necessities for complex and versatile microbial communities to exist. Evidence for biological material on several sites was also found previously in the form of chlorophylls, carotenoids, and pigments when using VNIR and Raman spectroscopy (Flahaut *et al.*, 2017).

The relative composition of the microbial communities in most samples follows a power-law distribution that is typically found in most soil samples, showing a relatively small number of highly dominant OTUs and a large number of low-abundant OTUs (Mandakovic *et al.*, 2018). The most dominant members of the communities observed in the salars are putative species that possess characteristics that would be expected in these environments such as extremely halophilic and acidophilic traits, spore-forming capabilities, and/or resistance against radiation and high or low temperatures. Members of the *Halobacteriaceae* family are often seen to dominate in highly saline environments (Mora-Ruiz *et al.*, 2018) and have previously been proposed as viable candidates when looking for (past) life on Mars due to their metabolic diversity and coping strategies with excessive salts (Oren, 2014).

A study focusing on the lake waters and the surrounding sediments of a salt lake in close proximity to the salars investigated in this study revealed dominant bacteria from the taxa of *Bacteriodetes*, *Proteobacteria*, and *Firmicutes* (Mandakovic *et al.*, 2018). No primers were used to amplify archaeal DNA. It is interesting to note that in terms of bacterial abundances, we also see these taxa as the dominant contributors to the bacterial communities. Further, many of the putative species detected in our study were also found in the study by Mandakovic *et al.* (2018) and show similar relative abundances. Cubillos *et al.* (2018) determined the prokaryotic communities in highly saline natural brines in the Salar de Atacama (close to our sampling sites) and found that these brines were strongly dominated by *Halobacteriaceae* with strong phylogenetic diversity, which matches well with our own observations. Interaction between these brines and the surface area may locally induce very high salinity and result in the more dominant presence of the extremely halophilic *Halobacteriaceae* species that we detected in these sediments. These studies seem to further suggest that microbial communities in the sediments of different salars in the region show strong similarities in terms of composition, which was also observed between the salars investigated in this study.

The low organic carbon content in most samples is in line with the expectations due to the region being notorious for having low carbon (Lester *et al.*, 2007; Azua-Bustos *et al.*, 2017). Organic carbon and nitrogen show a different distribution compared with the abundances of the amino acids in the soil samples. High amino acid load does not necessarily result in higher carbon or nitrogen values. This may be likely due to amino acids only forming a smaller fraction of the organic compounds that are present in most soils, and, therefore, their varying abundances are obscured. The weight percentage of total amino acids (using an average molecular weight of 120 Da) in our samples was found to be

on average about 20 times lower than organic carbon values. Considering the contribution of nitrogen, hydrogen, and oxygen to the molecular weight of amino acids as well, the contribution of amino acids to total organic carbon will be even lower. This phenomenon could explain that there is no correlation seen between amino acid abundances and organic carbon and nitrogen values.

Although not quantitatively, there is a trend observed where organic carbon values in the soil appears to reflect initial extractable DNA (whether this is prokaryotic or eukaryotic DNA). The largest fraction of the OTUs that are detected in the sequence results belongs to heterotrophic organisms, which rely on the presence of organic carbon for biomass production. Therefore, stronger presence of carbon in the soils would allow microbes to grow to increased densities, resulting in a higher retrievable fraction of DNA. However, Adonis tests showed that concentrations of organic carbon and nitrogen in the samples did not have a significant effect on the type of species present in the communities.

5. Conclusions

This study contributes to the ongoing expansion of our knowledge regarding the biological load in extreme environments that serve as Mars analogs. The salars investigated during this study were previously described as having a strong Mars analog potential due to the unique arid and volcanic environment of the region as well as the similarities in geological processes (Flahaut *et al.*, 2017). We found that microbial life was strongly represented in all salars and that the prokaryotic communities match previous observations. The communities show large contributions of (extremely) halophilic organisms as well as a relatively large number of species involved in the sulfur cycle, which is expected in an environment that is rich in salts and sulfates (*i.e.*, halite and gypsum).

Overall, a wide variety of microorganisms was found in these salars, which appear perfectly capable of surviving under the harsh conditions in one of the most extreme environments on Earth. However, there were clear differences observed between sample sites regarding the extractable biomass, suggesting that patchy distribution is still an issue to be considered. Samples with some of the highest biomass signatures were systematically found within relatively close proximity to (small) temporary bodies of water in the wetter margin areas.

The patchy nature of these salars did not allow us to appoint typical microbial communities per salar. Overall, different samples (from the same or from different salars) share a large number of species, although the abundances can differ dramatically. At the same time, there are many species (often less abundant) that are selectively represented in a subset of samples, which induces the variation we observe in the ordination plot. Small-scale variations in temperature, sediment composition, humidity, and sampling depth (among other parameters) likely play a role in the observed variations. However, differences in mineralogy between the sample sites (Flahaut *et al.*, 2017) did not explain the distributions observed in the microbial profiles. This is likely because most samples were seen to contain a mix of similar minerals and evaporites, although the relative contributions per site vary.

Brine types associated with the different salars may have influenced the number of different species (alpha diversity) that were detected since the salars fed by SO_4-rich brines had higher alpha diversity. SO_4-rich brines in the region likely result from extensive circulation in volcanic rocks in the subsurface, whereas Ca or mixed brines are proposed to result from circulation in the sedimentary bedrock, which in this area is mostly composed of sandstones and conglomerates (Risacher *et al.*, 2003). It may, therefore, be expected that SO_4-rich brines are richer in nutrients and could support a larger number of species (explaining the higher alpha diversity in these salars). However, Adonis tests did not result in significant *p*-values for the effect of brine type on the microbial distributions observed in the samples, suggesting that other environmental parameters exert stronger effects.

Amino acids and organic carbon and nitrogen found within the investigated soils match the microbial observations in that they generally correlate with the presence of pronounced life. Most samples showed considerable amounts of amino acids, of which the proteinogenic amino acids made up the bulk. The presence/absence, distribution, and enantiomeric excesses of these amino acids can be directly linked to the microbial life that is found within the samples, although a quantitative correlation could not be directly deduced. The same holds true for the organic carbon and nitrogen in the soils, which, though low in most samples, reflected to a certain extent the amount of genomic material that was recovered from the soils.

In addition to the observation that these salars are shown to support life to a large and diverse degree, there are other features that make these types of environments important targets for future Mars missions. Salts, such as halite and gypsum, that dominate these salars have strong preservation potential for biomarkers (Fernández-Remolar *et al.*, 2013; dos Santos *et al.*, 2016) and have been shown to be present on Mars, often in evaporitic contexts (Osterloo *et al.*, 2010; Flahaut *et al.*, 2014, 2015). If conditions on ancient Mars had allowed for microbial colonization in such environments, detectable remnants of these times are likely to have been preserved in the deeper layers of martian salt flats. Further, halite and/or gypsum depositions would be relatively easy to drill as opposed to harder materials in the martian regolith and would likely make good targets for future life detection missions to Mars aiming at drilling to the subsurface. Searching for organics at greater depths is widely considered a prerequisite, and it is also a main objective for ESA's ExoMars mission, since the surface of Mars has been exposed to billions of years of cosmic radiation (Pavlov *et al.*, 2002; Hassler *et al.*, 2014).

Due to the freezing temperatures on Mars, liquid water is expected to be present mainly as highly saturated brines. This is another strong argument for focusing on environments that are rich in salts when searching for traces of life. High concentrations of salts in water lower the freezing point substantially to around −50°C (Brass, 1980; Lide, 2004) and may allow certain analogies to extremely halophilic organisms such as *Halobacteriaceae* to survive in such brines, potentially making these types of environments some of the last potential habitats of current-day life on Mars. A member of the *Halobacteriaceae* family has previously been isolated from a hypersaline Antarctic lake (Franzmann *et al.*, 1988) and was shown to grow significantly at sub-zero temperatures (Reid *et al.*, 2006).

Downloaded by UPPSALA UNIVERSITETSBIBLIOTEK from www.liebertpub.com at 03/16/20. For personal use only.

Downloaded by UPPSALA UNIVERSITETSBIBLIOTEK from www.liebertpub.com at 03/16/20. For personal use only.

Author Disclosure Statement

No competing financial interests exist.

Funding Information

J.W. Aerts acknowledges the support from a grant from the User Support Programme Space Research (grant ALW-GO/13–09) of the Netherlands Organisation for Scientific Research (NWO). A.R. acknowledges the support from the European Union's Horizon 2020 research and innovation program under the Marie Skłodowska-Curie grant agreement No. 750353. J.F. was funded by an NWO VENI grant at the VU university Amsterdam at the time of the field expedition, and it is currently supported by CNRS and CNES at CRPG Nancy.

References

Aerts, J.W., Elsaesser, A., Roling, W.F.M., and Ehrenfreund, P. (2016) A contamination assessment of the CI carbonaceous meteorite Orgueil using a DNA-directed approach. *Meteorit Planet Sci* 51:920–931.

Amashukeli, X., Pelletier, C.C., Kirby, J.P., and Grunthaner, F.J. (2007) Subcritical water extraction of amino acids from Atacama Desert soils. *J Geophys Res* 112:G04S16.

Azua-Bustos, A., González-Silva, C., and Corsini, G. (2017) The hyperarid core of the Atacama Desert, an extremely dry and carbon deprived habitat of potential interest for the field of carbon science. *Front Microbiol* 8:993.

Berger, I.A. and Cooke, R.U. (1997) The origin and distribution of salts on alluvial fans in the Atacama Desert, Northern Chile. *Earth Surf Processes Landforms* 22:581–600.

Bibring, J.-P., Langevin, Y., Mustard, J.F., Poulet, F., Arvidson, R., Gendrin, A., Gondet, B., Mangold, N., Pinet, P., Forget, F., Berthé, M., Bibring J.-P., Gendrin, A., Gomez, C., Gondet, B., Jouglet, D., Poulet, F., Soufflot, A., Vincendon, M., Combes, M., Drossart, P., Encrenaz, T., Fouchet, T., Merchiorri, R., Belluci, G., Altieri, F., Formisano, V., Capaccioni, F., Cerroni, P., Coradini, A., Fonti, S., Korablev, O., Kottsov, V., Ignatiev, N., Moroz, V., Titov, D., Zasova, L., Loiseau, D., Mangold, N., Pinet, P., Douté, S., Schmitt, B., Sotin, C., Hauber, E., Hoffmann, H., Jaumann, R., Keller, U., Arvidson, R., Mustard, J.F., Duxbury, T., Forget, F., and Neukum, G. (2006) Global mineralogical and aqueous Mars history derived from OMEGA/Mars express data. *Science* 312:400–404.

Böhlke, J.K., Ericksen, G.E., and Revesz, K. (1997) Stable isotope evidence for an atmospheric origin of desert nitrate deposits in northern Chile and southern California, U.S.A. *Chem Geol* 136:135–152.

Bokulich, N.A., Subramanian, S., Faith, J.J., Gevers, D., Gordon, J.I., Knight, R., Mills, D.A., and Caporaso, J.G. (2013) Quality-filtering vastly improves diversity estimates from Illumina amplicon sequencing. *Nat Methods* 10:57–59.

Botta, O., Glavin, D.P., Kminek, G., and Bada, J.L. (2002) Relative amino acid concentrations as a signature for parent body processes of carbonaceous chondrites. *Orig Life Evol Biosph* 32:143–163.

Brass, G.W. (1980) Stability of brines on Mars. *Icarus* 42: 20–28.

Caporaso, J.G., Bittinger, K., Bushman, F.D., DeSantis, T.Z., Andersen, G.L., and Knight, R. (2009) PyNAST: a flexible tool for aligning sequences to a template alignment. *Bioinformatics* 26:266–267.

Caporaso, J.G., Kuczynski, J., Stombaugh, J., Bittinger, K., Bushman, F.D., Costello, E.K., Fierer, N., Pena, A.G., Goodrich, J.K., Gordon, J.I., Huttley, G.A., Kelley, S.T., Knights, D., Koenig, J.E., Ley, R.E., Lozupone, C.A., McDonald, D., Muegge, B.D., Pirrung, M., Reeder, J., Sevinsky, J.R., Turnbaugh, P.J., Walters, W.A., Widmann, J., Yatsunenko, T., Zaneveld, J., and Knight, R. (2010) QIIME allows analysis of high-throughput community sequencing data. *Nat Methods* 7:335–336.

Caporaso, J.G., Lauber, C.L., Walters, W.A., Berg-Lyons, D., Lozupone, C.A., Turnbaugh, P.J., Fierer, N., and Knight, R. (2011) Global patterns of 16S rRNA diversity at a depth of millions of sequences per sample. *Proc Natl Acad Sci U S A* 108:4516–4522.

Carr, M.H. (1996) Water on early Mars. *Ciba Found Symp* 202: 249–265; discussion 265–267.

Carr, M.H. and Head, J.W. (2010) Geologic history of Mars. *Earth Planet Sci Lett* 294:185–203.

Clarke, J.D.A. (2006) Antiquity of aridity in the Chilean Atacama Desert. *Geomorphology* 73:101–114.

Cordero, R.R., Damiani, A., Jorquera, J., Sepúlveda, E., Caballero, M., Fernandez, S., Feron, S., Llanillo, P.J., Carrasco, J., Laroze, D., and Labbe, F. (2018) Ultraviolet radiation in the Atacama Desert. *Antonie van Leeuwenhoek* 111:1301–1313.

Cubillos, C.F., Aguilar, P., Grágeda, M., and Dorador, C. (2018) Microbial communities from the world's largest lithium reserve, Salar de Atacama, Chile: life at high LiCl concentrations. *J Geophys Res Biogeosci* 123:3668–3681.

Direito, S.O.L., Marees, A., and Roling, W.F.M. (2012) Sensitive life detection strategies for low-biomass environments: optimizing extraction of nucleic acids adsorbing to terrestrial and Mars analogue minerals. *FEMS Microbiol Ecol* 81:111–123.

dos Santos, R., Patel, M., Cuadros, J., and Martins, Z. (2016) Influence of mineralogy on the preservation of amino acids under simulated Mars conditions. *Icarus* 277:342–353.

Edgar, R.C. (2010) Search and clustering orders of magnitude faster than BLAST. *Bioinformatics* 26:2460–2461.

Edgar, R.C. (2013) UPARSE: highly accurate OTU sequences from microbial amplicon reads. *Nat Methods* 10:996–998.

Ehlmann, B.L., Mustard, J.F., Murchie, S.L., Bibring, J.P., Meunier, A., Fraeman, A.A., and Langevin, Y. (2011) Subsurface water and clay mineral formation during the early history of Mars. *Nature* 479:53–60.

Ehrenfreund, P. and Charnley, S.B. (2000) Organic molecules in the interstellar medium, comets, and meteorites: a voyage from dark clouds to the early Earth. *Annu Rev Astron Astrophys* 38:427–483.

Ericksen, G.E. (1981) Geology and origin of the Chilean nitrate deposits. *U.S. Geol Surv Prof Pap* 37:1188.

Ericksen, G.E. (1983) The Chilean nitrate deposits: the origin of the Chilean nitrate deposits, which contain a unique group of saline minerals, has provoked lively discussion for more than 100 years. *Am Sci* 71:366–374.

Fernández-Remolar, D.C., Chong-Díaz, G., Ruíz-Bermejo, M., Harir, M., Schmitt-Kopplin, P., Tziotis, D., Gómez-Ortíz, D., García-Villadangos, M., Martín-Redondo, M.P., Gómez, F., Rodríguez-Manfredi, J.A., Moreno-Paz, M., De Diego-Castilla, G., Echeverría, A., Urtuvia, V.N., Blanco, Y., Rivas, L., Izawa, M.R.M., Banerjee, N.R., Demergasso, C., and Parro, V. (2013) Molecular preservation in halite- and perchlorate-rich hypersaline subsurface deposits in the Salar Grande basin (Atacama Desert, Chile): implications for the search for molecular biomarkers on Mars. *J Geophys Res Biogeosci* 118:922–939.

Downloaded by UPPSALA UNIVERSITETSBIBLIOTEK from www.liebertpub.com at 03/16/20. For personal use only.

Flahaut, J., Massé, M., Le Deit, L., Thollot, P., Bibring, J.P., Poulet, F., Quantin, C., Mangold, N., Michalski, J., and Bishop, J.L. (2014) Sulfate-rich deposits on Mars: a review of their occurences and geochemical implications. In *Eighth International Conference on Mars*, LPI Contributions, Pasadena, CA, 1791, p. 1196.

Flahaut, J., Carter, J., Poulet, F., Bibring, J.P., van Westrenen, W., Davies, G.R., and Murchie, S.L. (2015) Embedded clays and sulfates in Meridiani Planum, Mars. *Icarus* 248:269–288.

Flahaut, J., Martinot, M., Bishop, J.L., Davies, G.R., and Potts, N.J. (2017) Remote sensing and in situ mineralogic survey of the Chilean salars: an analog to Mars evaporate deposits? *Icarus* 282:152–173.

Franzmann, P.D., Stackebrandt, E., Sanderson, K., Volkman, J.K., Cameron, D.E., Stevenson, P.L., McMeekin, T.A., and Burton, H.R. (1988) Halobacterium lacusprofundi sp. nov., a halophilic bacterium isolated from Deep Lake, Antarctica. *Syst Appl Microbiol* 11:20–27.

Gendrin, A., Mangold, N., Bibring J.-P., Langevin, Y., Gondet, B., Poulet, F., Bonello, G., Quantin, C., Mustard, J., Arvidson, R., and LeMouélic, S. (2005) Sulfates in martian layered terrains: the OMEGA/Mars express view. *Science* 307:1587–1591.

Gómez-Silva, B., Rainey, F.A., Warren-Rhodes, K.A., McKay, C.P., and Navarro-González, R. (2008) Atacama Desert soil microbiology. In *Microbiology of Extreme Soils*, edited by P. Dion and C.S. Nautiyal, Springer Berlin Heidelberg, Berlin, Heidelberg, pp 117–132.

Grotzinger, J.P., Sumner, D.Y., Kah, L.C., Stack, K., Gupta, S., Edgar, L., Rubin, D., Lewis, K., Schieber, J., Mangold, N., Milliken, R., Conrad, P.G., DesMarais, D., Farmer, J., Siebach, K., Calef, F., Hurowitz, J., McLennan, S.M., Ming, D., Vaniman, D., Crisp, J., Vasavada, A., Edgett, K.S., Malin, M., Blake, D., Gellert, R., Mahaffy, P., Wiens, R.C., Maurice, S., Grant, J.A., Wilson, S., Anderson, R.C., Beegle, L., Arvidson, R., Hallet, B., Sletten, R.S., Rice, M., Bell, J., Griffes, J., Ehlmann, B., Anderson, R.B., Bristow, T.F., Dietrich, W.E., Dromart, G., Eigenbrode, J., Fraeman, A., Hardgrove, C., Herkenhoff, K., Jandura, L., Kocurek, G., Lee, S., Leshin, L.A., Leveille, R., Limonadi, D., Maki, J., McCloskey, S., Meyer, M., Minitti, M., Newsom, H., Oehler, D., Okon, A., Palucis, M., Parker, T., Rowland, S., Schmidt, M., Squyres, S., Steele, A., Stolper, E., Summons, R., Treiman, A., Williams, R., Yingst, A., and MSL Science Team. (2014) A habitable fluvio-lacustrine environment at Yellowknife Bay, Gale Crater, Mars. *Science* 343:1242777.

Hand, K.P., Murray, A.E., Garvin, J.B., Brinckerhoff, W.B., Christner, B.C., Edgett, K.S., Ehlmann, G.L., German, C.R., Hayes, A.G., Hoehler, T.M., Horst, S.M., Lunine, J.I., Nealson, K.H., Paranicas, C., Schmidt, B.E., Smith, D.E., Rhoden, A.R., Russell, M.J., Templeton, A.D., Willis, P.A., Yingst, R.A., Phillips, C.B., Cable, M.L., Craft, K.L., Hofmann, A.E., Nordheim, T.A., Pappalardo, R.P., and the Project Engineering Team. (2017) Report of the Europa Lander Science Definition Team, JPL publication D-97667, Jet Propulsion Laboratory, Pasadena, CA. https://isulibrary.isunet.edu/index.php?lvl=notice_display&id=10061

Hassler, D.M., Zeitlin, C., Wimmer-Schweingruber, R.F., Ehresmann, B., Rafkin, S., Eigenbrode, J.L., Brinza, D.E., Weigle, G., Böttcher, S., Böhm, E., Burmeister, S., Guo, J., Köhler, J., Martin, C., Reitz, G., Cucinotta, F.A., Kim M.-H., Grinspoon, D., Bullock, M.A., Posner, A., Gómez-Elvira, J., Vasavada, A., Grotzinger, J.P., and MSL Science Team. (2014) Mars' surface radiation environment measured with the Mars Science Laboratory's Curiosity rover. *Science* 343:1244797.

Herlemann, D.P.R., Labrenz, M., Jurgens, K., Bertilsson, S., Waniek, J.J., and Andersson, A.F. (2011) Transitions in bacterial communities along the 2000 km salinity gradient of the Baltic Sea. *ISME J* 5:1571–1579.

Higgs, P.G. and Pudritz, R.E. (2009) A Thermodynamic basis for prebiotic amino acid synthesis and the nature of the first genetic code. *Astrobiology* 9:483–490.

Hunter, C.N., Daldal, F., Thurnauer, M.C., and Beaty, J.T. (2008) *The Purple Phototrophic Bacteria*. Springer, New York City.

Hynek, B.M., Beach, M., and Hoke, M.R.T. (2010) Updated global map of Martian valley networks and implications for climate and hydrologic processes. *J Geophys Res Planets* 115:E09008.

Kozlowski, L.P. (2016) Proteome-pI: proteome isoelectric point database. *Nucleic Acids Res* 45:D1112–D1116.

Lester, E.D., Satomi, M., and Ponce, A. (2007) Microflora of extreme arid Atacama Desert soils. *Soil Biol Biochem* 39:704–708.

Lide, R.D. (2004) *CRC Handbook of Chemistry and Physics*. CRC press, Boca Raton, FL, pp 2712.

Mandakovic, D., Maldonado, J., Pulgar, R., Cabrera, P., Gaete, A., Urtuvia, V., Seeger, M., Cambiazo, V., and González, M. (2018) Microbiome analysis and bacterial isolation from Lejía Lake soil in Atacama Desert. *Extremophiles* 22:665–673.

Martin, M. (2011) Cutadapt removes adapter sequences from high-throughput sequencing reads. *EMBnet J* 17:10–12.

Martins, Z., Botta, O., and Fogel, M.L. (2008) Extraterrestrial nucleobases in the Murchison meteorite. *Earth Planet Sci Lett* 270:130–136.

Masella, A.P., Bartram, A.K., Truszkowski, J.M., Brown, D.G., and Neufeld, J.D. (2012) PANDAseq: paired-end assembler for illumina sequences. *BMC Bioinformatics* 13:31.

McDonald, D., Clemente, J.C., Kuczynski, J., Rideout, J.R., Stombaugh, J., Wendel, D., Wilke, A., Huse, S., Hufnagle, J., Meyer, F., Knight, R., and Caporaso, J.G. (2012) The Biological Observation Matrix (BIOM) format or: how I learned to stop worrying and love the ome-ome. *Gigascience* 1:7.

McKay, C.P., Friedmann, E.I., Gómez-Silva, B., Cáceres-Villanueva, L., Andersen, D.T., and Landheim, R. (2003) Temperature and moisture conditions for life in the extreme arid region of the Atacama Desert: four years of observations including the El Niño of 1997–1998. *Astrobiology* 3:393–406.

Meierhenrich, U.J. (2008) *Amino Acids and the Asymmetry of Life*. Springer, New York City.

Meinert, C. and Meierhenrich, U.J. (2012) A new dimension in separation science: comprehensive two-dimensional gas chromatography. *Angew Chem Int Ed* 51:10460–10470.

Michalski, G., Böhlke, J.K., and Thiemens, M. (2004) Long term atmospheric deposition as the source of nitrate and other salts in the Atacama Desert, Chile: new evidence from mass-independent oxygen isotopic compositions. *Geochim Cosmochim Acta* 68:4023–4038.

Mora-Ruiz, M.D.R., Cifuentes, A., Font-Verdera, F., Pérez-Fernández, C., Farias, M.E., González, B., Orfila, A., and Rosselló-Móra, R. (2018) Biogeographical patterns of bacterial and archaeal communities from distant hypersaline environments. *Syst Appl Microbiol* 41:139–150.

Murchie, S.L., Mustard, J.F., Ehlmann, B.L., Milliken, R.E., Bishop, J.L., McKeown, N.K., Noe Dobrea, E.Z., Seelos, F.P., Buczkowski, D.L., Wiseman, S.M., Arvidson, R.E., Wray, J.J., Swayze, G., Clark, R.N., Des Marais, D.J., McEwen, A.S., and Bibring J.-P. (2009) A synthesis of Martian aqueous mineralogy after 1 Mars year of observations from the Mars Reconnaissance Orbiter. *J Geophys Res Planets* 114:E00D06.

Mustard, J.F., Murchie, S.L., Pelkey, S.M., Ehlmann, B.L., Milliken, R.E., Grant, J.A., Bibring, J.P., Poulet, F., Bishop, J., Dobrea, E.N., Roach, L., Seelos, F., Arvidson, R.E., Wiseman, S., Green, R., Hash, C., Humm, D., Malaret, E., McGovern, J.A., Seelos, K., Clancy, T., Clark, R., Marais, D.D., Izenberg, N., Knudson, A., Langevin, Y., Martin, T., McGuire, P., Morris, R., Robinson, M., Roush, T., Smith, M., Swayze, G., Taylor, H., Titus, T., and Wolff, M. (2008) Hydrated silicate minerals on Mars observed by the Mars Reconnaissance Orbiter CRISM instrument. *Nature* 454:305–309.

Muyzer, G., Dewaal, E.C., and Uitterlinden, A.G. (1993) Profiling of complex microbial-populations by denaturing gradient gel-electrophoresis analysis of polymerase chain reaction-amplified genes-coding for 16s ribosomal-RNA. *Appl Environ Microbiol* 59:695–700.

Navarro-Gonzalez, R., Rainey, F.A., Molina, P., Bagaley, D.R., Hollen, B.J., de la Rosa, J., Small, A.M., Quinn, R.C., Grunthaner, F.J., Caceres, L., Gomez-Silva, B., and McKay, C.P. (2003) Mars-like soils in the Atacama Desert, Chile, and the dry limit of microbial life. *Science* 302:1018–1021.

Nimura, N. and Kinoshita, T. (1986) o-Phthalaldehyde—N-acetyl-L-cysteine as a chiral derivatization reagent for liquid chromatographic optical resolution of amino acid ernantiomers and its application to conventional amino acid analysis. *J Chromatogr A* 352:169–177.

Oren, A. (2014) Halophilic archaea on Earth and in space: growth and survival under extreme conditions. *Philos Trans R Soc A Math Phys Eng Sci* 372:20140194.

Osterloo, M., Scott Anderson, F., Hamilton, V.E., and Hynek, B.M. (2010) The geologic context of chloride-bearing materials on Mars. *J Geophys Res* 115:E10012

Osterloo, M.M., Hamilton, V.E., Bandfield, J.L., Glotch, T.D., Baldridge, A.M., Christensen, P.R., Tornabene, L.L., and Anderson, F.S. (2008) Chloride-bearing materials in the southern highlands of Mars. *Science* 319:1651–1654.

Parro, V., de Diego-Castilla, G., Moreno-Paz, M., Blanco, Y., Cruz-Gil, P., Rodriguez-Manfredi, J.A., Fernandez-Remolar, D., Gomez, F., Gomez, M.J., Rivas, L.A., Demergasso, C., Echeverria, A., Urtuvia, V.N., Ruiz-Bermejo, M., Garcia-Villadangos, M., Postigo, M., Sanchez-Roman, M., Chong-Diaz, G., and Gomez-Elvira, J. (2011) A microbial oasis in the hypersaline Atacama subsurface discovered by a life detector chip: implications for the search for life on Mars. *Astrobiology* 11:969–996.

Patzelt, D.J., Hodač, L., Friedl, T., Pietrasiak, N., and Johansen, J.R. (2014) Biodiversity of soil cyanobacteria in the hyperarid Atacama Desert, Chile. *J Phycol* 50:698–710.

Pavlov, A.K., Blinov, A.V., and Konstantinov, A.N. (2002) Sterilization of Martian surface by cosmic radiation. *Planet Space Sci* 50:669–673.

Pollack, J.B., Kasting, J.F., Richardson, S.M., and Poliakoff, K. (1987) The case for a wet, warm climate on early Mars. *Icarus* 71:203–224.

Poulet, F., Bibring, J.P., Mustard, J.F., Gendrin, A., Mangold, N., Langevin, Y., Arvidson, R.E., Gondet, B., Gomez, C., Berthe, M., Erard, S., Forni, O., Manaud, N., Poulleau, G., Soufflot, A., Combes, M., Drossart, P., Encrenaz, T., Fouchet, T., Melchiorri, R., Bellucci, G., Altieri, F., Formisano, V., Fonti, S., Capaccioni, F., Cerroni, P., Coradini, A., Korablev, O., Kottsov, V., Ignatiev, N., Titov, D., Zasova, L., Pinet, P., Schmitt, B., Sotin, C., Hauber, E., Hoffmann, H., Jaumann, R., Keller, U., and Forget, F. (2005) Phyllosilicates on Mars and implications for early martian climate. *Nature* 438:623–627.

Price, M.N., Dehal, P.S., and Arkin, A.P. (2009) FastTree: computing large minimum evolution trees with profiles instead of a distance matrix. *Mol Biol Evol* 26:1641–1650.

Pylro, V.S., Roesch, L.F.W., Morais, D.K., Clark, I.M., Hirsch, P.R., and Totola, M.R. (2014) Data analysis for 16S microbial profiling from different benchtop sequencing platforms. *J Microbiol Methods* 107:30–37.

Quast, C., Pruesse, E., Yilmaz, P., Gerken, J., Schweer, T., Yarza, P., Peplies, J., and Glockner, F.O. (2013) The SILVA ribosomal RNA gene database project: improved data processing and web-based tools. *Nucleic Acids Res* 41:D590–D596.

Quinn, R.C., Martucci, H.F.H., Miller, S.R., Bryson, C.E., Grunthaner, F.J., and Grunthaner, P.J. (2013) Perchlorate radiolysis on Mars and the origin of martian soil reactivity. *Astrobiology* 13:515–520.

Reid, I.N., Sparks, W.B., Lubow, S., McGrath, M., Livio, M., Valenti, J., Sowers, K.R., Shukla, H.D., MacAuley, S., Miller T., Suvanasuthi, R., Belas, R., Colman, A., Robb, F.T., DasSarma, P., Müller, J.A., Coker, J.A., Cavicchioli, R., Chen, F., and DasSarma, S. (2006) Terrestrial models for extraterrestrial life: methanogens and halophiles at Martian temperatures. *Int J Astrobiol* 5:89–97.

Risacher, F., Alonso, H., and Salazar, C. (2003) The origin of brines and salts in Chilean salars: a hydrochemical review. *Earth Sci Rev* 63:249–293.

Skelley, A.M., Scherer, J.R., Aubrey, A.D., Grover, W.H., Ivester, R.H.C., Ehrenfreund, P., Grunthaner, F.J., Bada, J.L., and Mathies, R.A. (2005) Development and evaluation of a microdevice for amino acid biomarker detection and analysis on Mars. *Proc Natl Acad Sci U S A* 102:1041–1046.

Squyres, S.W., Grotzinger, J.P., Arvidson, R.E., Bell, J.F., 3rd, Calvin, W., Christensen, P.R., Clark, B.C., Crisp, J.A., Farrand, W.H., Herkenhoff, K.E., Johnson, J.R., Klingelhofer, G., Knoll, A.H., McLennan, S.M., McSween, H.Y., Jr., Morris, R.V., Rice, J.W., Jr., Rieder, R., and Soderblom, L.A. (2004) In situ evidence for an ancient aqueous environment at Meridiani Planum, Mars. *Science* 306:1709–1714.

Stoertz, G.E. and Ericksen, G.E. (1974) Geology of salars in Northern Chile (811). *U.S. Geol Surv Prof Pap* 811:65.

Sutter, B., Dalton, J.B., Ewing, S.A., Amundson, R., and McKay, C.P. (2007) Terrestrial analogs for interpretation of infrared spectra from the Martian surface and subsurface: sulfate, nitrate, carbonate, and phyllosilicate-bearing Atacama Desert soils. *J Geophys Res Biogeosci* 112:4.

Vago, J.L., Westall, F., Coates, A.J., Jaumann, R., Korablev, O., Ciarletti, V., Mitrofanov, I., Josset J.-L., De Sanctis, M.C., Bibring J.-P., Rull, F., Goesmann, F., Steininger, H., Goetz, W., Brinckerhoff, W., Szopa, C., Raulin, F., Westall, F., Edwards, H.G.M., Whyte, L.G., Fairén, A.G., Bibring J.-P., Bridges, J., Hauber, E., Ori, G.G., Werner, S., Loizeau, D., Kuzmin, R.O., Williams, R.M.E., Flahaut, J., Forget, F., Vago, J.L., Rodionov, D., Korablev, O., Svedhem, H., Sefton-Nash, E., Kminek, G., Lorenzoni, L., Joudrier, L., Mikhailov, V., Zashchirinskiy, A., Alexashkin, S., Calantropio, F., Merlo, A., Poulakis, P., Witasse, O., Bayle, O., Bayón, S., Meierhenrich, U., Carter, J., García-Ruiz, J.M., Baglioni, P., Haldemann, A., Ball, A.J., Debus, A., Lindner, R., Haessig, F., Monteiro, D., Trautner, R., Voland, C., Rebeyre, P., Goulty, D., Didot, F., Durrant, S., Zekri, E., Koschny, D., Toni, A., Visentin, G., Zwick, M., van Winnendael, M., Azkarate, M., and Carreau, C. (2017) Habitability on early Mars and the search for biosignatures with the ExoMars rover. *Astrobiology* 17:471–510.

Downloaded by UPPSALA UNIVERSITETSBIBLIOTEK from www.liebertpub.com at 03/16/20. For personal use only.

Warren-Rhodes, K.A., Rhodes, K.L., Pointing, S.B., Ewing, S.A., Lacap, D.C., Gomez-Silva, B., Amundson, R., Friedmann, E.I., and McKay, C.P. (2006) Hypolithic cyanobacteria, dry limit of photosynthesis, and microbial ecology in the hyperarid Atacama Desert. *Microb Ecol* 52:389–398.

Yilmaz, P., Parfrey, L.W., Yarza, P., Gerken, J., Pruesse E., Quast C., Schweer T., Peplies J., Ludwig W., and Glöckner, F.O. (2014) The SILVA and ''All-species Living Tree Project (LTP)'' taxonomic frameworks. *Nucleic Acids Res* 42:D643–D648.

Address correspondence to:
Joost W. Aerts
Molecular Cell Biology
Faculty of Science
VU University Amsterdam
Amsterdam 1081 HV
The Netherlands

E-mail: joost.w.aerts@gmail.com

Submitted 9 March 2019
Accepted 12 November 2019

Abbreviations Used

ASTER = Advanced Spaceborne Thermal Emission and Reflection Radiometer
BIOM = Biological Observation Matrix
CN = Carbon-Nitrogen
ECHFBE = N-ethoxycarbonyl heptafluorobutyl ester
GC = gas chromatography
GC × GC-MS = Multidimensional Gas Chromatography Mass Spectrometry
HEPA = High-Efficiency-Particulate-Air
LC-MS = liquid chromatography/mass spectrometry
OPA/NAC = o-phthaldialdehyde/N-acetyl-L-cysteine
OTUs = operational taxonomic units
PCR = polymerase chain reaction
QIIME = Quantitative Insights Into Microbial Ecology (a bioinformatic pipeline)
ULC/MS = ultra-high-performance liquid chromatography/mass spectrometry
UV = ultraviolet
VNIR = visible and near infrared

Downloaded by UPPSALA UNIVERSITETSBIBLIOTEK from www.liebertpub.com at 03/16/20. For personal use only.